

The Economic Linkages of Covid-19 Across Sectors and Regions in the UK*

Fidel Pérez-Sebastián[†]

Rafael Serrano-Quintero[‡]

Abstract

This paper builds a spatial model of trade with supply-chain links to try to understand the effect of economic links and policies on the spread of the Covid-19 pandemic during the first wave across NUTS2 UK regions. We find that the fight to reduce infection rates was more successful in the UK than in the European Union. Our results imply that without the policy reaction in Europe, the number of deaths during the first wave of the pandemic would have been about 4,400,000 larger in the European Union and about 1,217,000 higher in the UK, and that these benefits vary greatly across UK regions. Comparing the effects of the policies implemented in the EU27 and in the UK, we estimate that, in the absence of European-Union's anti-Covid-19 measures, the number of deaths in the UK would have been an 80% larger; and that UK anti-Covid-19 measures saved about 50,000 lives in the European Union and 1,200,000 lives in the UK.

JEL Classification: E10, I10, R10

Keywords: Spatial Economics, Covid-19, first wave, policy response, quantitative models.

1 Introduction

The recent COVID-19 pandemic has ended 4.55 million lives (as of October 1st, 2021), forced quarantines all over the world, stopped global value chains for a significant amount of time, and created one of the largest global recessions in recent years. However, as with the spread of other infectious diseases, its impact in terms of lives and economic activity has varied greatly across regions and industries (see, e.g., [Villani, McKee, Cascini, Ricciardi, and Boccia \(2020\)](#) and [de Vet, Nigohosyan, Ferrer, Gross, Kuehl, and Flickenschild \(2021\)](#)). In this paper, we build on the idea that diffusion of infectious diseases depend on human interactions (e.g., see [Fogli and Veldkamp \(2021\)](#)), and in particular, on how dense is the economic network of a given area. We consider endogenously determined economic interactions and analyze the effect of the policies adopted to fight the first wave of the pandemic across different regions in the UK. More specifically, the paper asks the following questions. What is the contribution of economic linkages to the expansion of the disease? How many lives have the polices implemented saved?

*Fidel Pérez Sebastián acknowledges financial support from ESRC-UKRI under grant ES/V015265/1.

[†]Faculty of Business, Law and Politics, University of Hull, UK; and FAE, Universidad de Alicante, Spain. E-mail: fidel.perez.sebastian@gmail.com.

[‡]Department of Economic Theory, Universitat de Barcelona, Spain. E-mail: rafael.serrano@ub.edu

The model we develop embeds an spatial economic model in the spirit of [Allen and Arkolakis \(2014\)](#); [Caliendo and Parro \(2014\)](#) and [Caliendo, Parro, Rossi-Hansberg, and Sarte \(2017\)](#) into the canonical Susceptible, Infected, Recovered (SIR) model by [Kermack, McKendrick, and Walker \(1927\)](#). The purpose of the proposed framework is to analyze the two way causation between the spatial dynamics of an epidemic and the spatial distribution of economic activity. More specifically, the setup incorporates Ricardian trade *à la* [Eaton and Kortum \(2002\)](#), and extends the SIR model in two ways. First, similar to [Fernandez-Villaverde and Jones \(2020\)](#), we consider five population groups composed of susceptible, vaccinated, infected, resolving, and recovered individuals, and also account for deaths. Second, we allow for spatial connections that are endogenously determined by the structure of our economic geography model. The assumption is that when regions trade, people enter in contact with one another so they put themselves at risk of getting infected or that the virus is itself transported through the imported goods. As a result of the economic geography model, denser regions will experience more rapid increase in infections for two reasons. First, within the region, there are more interactions across individuals and thus, a higher probability of transmission. Second, the larger a region is, the more it will trade with other regions, and thus, the higher the probability of transmitting the disease across regions.

In our framework, the economy is composed of a set of locations that produce goods in different sectors. Each sector produces three goods: a final product, an intermediate good, and a composite intermediate or material. The first two can be traded but trade is costly. The third one is only sold domestically within the region. In addition, following [Caliendo and Parro \(2014\)](#), whereas the domestic movement of materials is inter-industry, cross-regional trade of intermediate goods is purely intra-industry.¹ This feature captures that the latter type of trade represents the largest component of the trade flows of intermediates. For example, [World Bank \(2009\)](#) finds that, from 1962 to 2006, worldwide intra-industry trade in intermediate goods increased approximately from 30% to 60% of total trade. This share equals 42 percent in our European Union 28-country group (EU28) dataset for the year 2013. What is most important is that these inter- and intra-industry links across sectors mean that policies and changes that affect a given industry can potentially affect all other sectors and regions. Our main contribution is to assess how the heterogeneity in production structures and regional connections affect the spread of the disease and its economic impact.

The model proceeds in two phases. For a given the population composition, the first phase obtains the distribution of economic activity and bilateral trade shares. In the second phase, we take as given the bilateral trade shares and the spatial distribution of economic activity along with the disease ecology to determine how the population composition changes from one week to the next. This

¹ Compared to the sectoral structure presented by [Caliendo and Parro \(2014\)](#), the main difference with ours is that we consider that final consumption products can cross regional borders. The reason is that some of them, like tourism, can be important for the propagation of the virus and are tradable.

creates a loop in which disease dynamics and economic activity affect each other. In particular, disease prevalence can reduce the labor force in a region through either mortality, morbidity or policy actions. These shocks affect the level of economic activity and reduce international trade. The modification of the trade patterns, in turn, has an impact on the spread of the disease by decreasing the amount of infection “*exported*” to other regions. These general equilibrium forces resemble a behavioral response in which agents protect themselves from the infection.

The explicit modelling of the geography is important to understand the disease dynamics.² In general, those regions that are more isolated will receive and transmit less the infection. As an example, take the evolution of the pandemic in Spain versus Italy and the UK. The spread of the infection in Spain was faster in Madrid (a region in the center of the country) and then expanded throughout the nation. In Italy, the infection started in the north and then moved slowly towards the south. In the UK, in turn, the disease was more concentrated in the south but, at the same time, more widespread than in other parts of Europe. Our model addresses these singularities through the explicit modelling of the geography of trade in Europe.

We calibrate the model to match the distribution of workers and wages across 230 regions from 28 countries in Europe for 10 sectors of production comprising the whole economy and use our framework to assess through a set of counterfactuals, how policies adopted during the coronavirus pandemic, which include social distancing and regional lockdowns, have affected the impact of the disease. We focus on the first wave that goes from February 25th to July 15th, 2020.

We find that, even though the incidence of the disease was larger in the UK than in the European Union, the fight to reduce the infection rates was more successful in the former economy than in the latter. Our results also imply that without the policy reaction in Europe, the number of deaths during the first wave of the pandemic would have been about 4,400,000 larger in the European Union and about 1,217,000 higher in the UK, and that these benefits greatly vary across UK regions. Comparing the effects of the policies implemented in the EU27 and in the UK, we estimate that, in the absence of European-Union’s anti-Covid-19 measures, the number of deaths in the UK would have been an 80% larger, which would have implied 34 additional deaths per 100,000 inhabitants. Finally, UK anti-Covid-19 measures saved 50,620 lives in the European Union and about 1,200,000 lives in the UK.

The paper proceeds as follows. Section 2 describes the related literature. Section 3 introduces the model. The calibration of its exogenous variables and parameters is discussed in section 4. Section 5 presents the results. Section 6 concludes.

²Wilson (2010) surveys the literature on the links between geography and infectious diseases and notes that socioeconomic conditions, public health infrastructure, urban versus rural environments, density and mobility of the population are important factors explaining the types and abundance.

2 Related Literature

Our paper contributes to a large and growing literature on the economic interactions and infectious diseases. We motivate our modelling strategy based on the empirical evidence supporting the link between economic interactions and infectious diseases. Several early examples showed the importance of diseases in developing countries. [Chakraborty, Papageorgiou, and Pérez-Sebastián \(2010\)](#) introduce rational disease behavior in a general equilibrium framework focused on the effects of the burden of malaria and the HIV infection on economic development. They show that these diseases can be a source of economic growth traps. [Oster \(2012\)](#), it turn, shows in the context of Africa, that engaging in exports leads to a large and significant increase in new HIV infections mainly due to the movement of truckers.

The connection between trade and infectious-disease transmission is not only prevalent in developing countries. [Adda \(2016\)](#) provides evidence based on microdata that the expansion of transportation networks and interregional trade had a significant impact on virus spreading in France. Focusing on European pandemics going back to the 14th century, [Jorda, Singh, and Taylor \(2020\)](#) find important long-run economic consequences even after 40 years. In the context of COVID-19 in the United States, [Desmet and Wacziarg \(2021\)](#) show that population density of a county is persistently correlated with its COVID-19 severity. We contribute to this strand of the literature by constructing and calibrating a model for a set of European regions at different stages of development and assessing the importance of trade on the spread of the disease.

We are not the first in introducing spatial connections in epidemiological models. [Lloyd and May \(1996\)](#) and [Keeling \(1999\)](#) are early examples of spatial models of epidemics. [Paeng and Lee \(2017\)](#) extend the canonical SIR model by including spatial infections assuming that the infection can be spread in a given radius. In the epidemiological literature, the connection between trade and the spread of infectious diseases is also known, [Mayer \(2000\)](#) notes that vectors of transmission of dengue fever or cholera were introduced in the U.S. through imported tires and through dumping bilge water into the ocean. We depart from this literature by endogenizing the spatial connections within a quantitative economic geography model, instead of assuming a given radius of infection or stochastic encounters.

More closely related to our context, [Antràs, Redding, and Rossi-Hansberg \(2020\)](#) build a two-country framework of human interactions in which they combine a gravity equation structure and an epidemiological model of disease evolution. In their model, the disease spreads as agents travel from one country to another. We depart from them by building a multi-country and multi-sector setup with an input-output structure rich enough to capture the transmission of the disease through bilateral trade across all the network nodes. The inclusion of different sectors can also allow us to

consider a wider array of policies, like selected closures.

We use our model to address the effect of region-specific lockdown policies during the first wave of the pandemic and the trade-off between the spread of the disease and potential losses from not engaging in trade. Recent papers study optimal lockdown policies focusing on different group populations (Acemoglu, Chernozhukov, Werning, and Whinston, 2020), the intensity and duration of the policy (Alvarez, Argente, and Lippi, 2020), and the distributional consequences (Glover, Heathcote, Krueger, and Rios-Rull, 2020). More closely to our context, Fajgelbaum, Khandelwal, Kim, Mantonvini, and Schaal (2020) find that regional-specific lockdowns result in better outcomes than uniform lockdowns. We depart from them by analyzing the policy effects at a higher regional level, but our result go in line with theirs. We also depart from them in that we consider deaths as a crucial vector affecting the labor supply.

Our article also talks to another branch of recent papers focused on consumer behavior and output responses when faced with an infectious disease (Eichenbaum, Rebelo, and Trabandt, 2020; Guerrieri, Lorenzoni, Straub, and Werning, 2020; Krueger, Uhlig, and Xie, 2020). Crucially, we depart from them by looking at the differential effects of having an open economy, multiple regions, and a rich input-output structure. Çakmaklı, Demiralp, Kalemli-Özcan, Yeşiltaş, and Yıldırım (2021) study how demand and supply shocks affect global vaccinations and how vaccinations of other countries can potentially benefit home countries. They do not include, however, endogenous links for the spread of the infection. We also extend the methodology by Fernandez-Villaverde and Jones (2020) to recover infection rates based on future deaths and use it to calibrate our model with endogenous links in the disease.

3 The model

We assume the economy is composed of a set of G geographical locations or regions that belong to different countries and J sectors or industries. Regions are denoted by g , i and h and sectors by j and k . In each industry, there is production of a composite intermediate or material, an array of different varieties of intermediate goods, and a set of different types of final consumption goods. Households provide labor to the production process. Labor is mobile across sectors and immobile across locations. All markets are perfectly competitive.

We abstract from the movement of workers across locations, because this aspect does not seem to have played a significant role during the pandemic due, among other things, to the mobility restrictions imposed. In the model, the effect of the movement of people to the spread of the virus will be captured by the level of activity in sectors related to transportation and tourism.

The model offers a rich supply chain structure. Local materials from different sectors are employed

along with the labor input to produce intermediate goods. In the next stage, intermediate goods produced by the same industry possibly in different locations are combined to generate final consumption products and a composite intermediate or material. These connections among the different stages of the production chain can provide amplification effects of trade disruptions.

We suppose that the intermediate goods and final products can be tradable or not, whereas materials are not tradable. We consider that final consumption products can cross regional borders, because some of them, like tourism, can be important for the propagation of the virus and are tradable. Trade in intermediate goods is intra-industry, which represents the largest component of the world trade flows of intermediates.

Let us now move to describing the model demographics. For simplicity, we omit time subscripts. The size of the population in region g equals N_g . This population is composed of five groups: susceptible vaccinated and susceptible non-vaccinated people—denoted by V_g and S_g , respectively—who are not infected but can develop the disease; infected individuals, I_g ; resolving cases R_g who can pass away with probability δ or recover with probability $(1 - \delta)$; ³ and recovered C_g , who can potentially get reinfected. Hence, it must be satisfied that

$$N_g = S_g + V_g + I_g + R_g + C_g. \quad (1)$$

We will consider the possibility that recovered and vaccinated individuals may rejoin the susceptible non-vaccinated population once the partial immunity acquired by being exposed to the virus or the vaccine is lost.

Only a fraction l_{gH} from each group H can supply labor services. This fraction l_{gH} will be taken as exogenous, given by morbidity and policy considerations. Then, the available labor force L_g equals:

$$L_g = l_{gS}S_g + l_{gV}V_g + l_{gI}I_g + l_{gR}R_g + l_{gC}C_g. \quad (2)$$

With these ingredients, the model can be numerically solved through a loop that consists of two phases. In the first phase, given the population composition, we can obtain the spatial distribution of economic activity. The second phase takes as given the spatial distribution delivered by the first phase, along with the disease ecology to determine how the population composition changes from one day to the next. We consider that the infection can spread within and across locations because of people contact. Finally, the new population composition feeds again the first phase, and this loop continues until predictions for the desired number of weeks are generated.

³Resolving cases are infected individuals that cannot infect other people. [Fernandez-Villaverde and Jones \(2020\)](#) suggest that distinguishing between infection and recovery periods matters for the model to fit the data well with biologically sensible parameters.

3.1 Phase 1: Economic Allocations Across Space

The first phase of the model determines the underlying economic geography through which the virus and the economic consequences of policies will potentially spread.

3.1.1 Households

Welfare-maximizing consumers in each location have identical preferences given by:⁴

$$W_g = \prod_{j=1}^J (c_g^j)^{\alpha_g^j}; \quad (3)$$

where

$$c_g^j = \left[\int_0^1 c_g^j(\Omega^j)^{1-1/\varsigma^j} d\Omega^j \right]^{\varsigma^j/(\varsigma^j-1)}; \quad (4)$$

the parameter α_g^j represents the share of sector- j products in total consumption expenditure in location g , that is, $\sum_{j=1}^J \alpha_g^j = 1$; the variable $c_g^j(\Omega^j)$ denotes the units consumed in location g of variety Ω^j from sector- j (Ω^j is one among a mass of size *one* of different varieties); and the parameter ς^j gives the elasticity of substitution between different varieties of sector- j consumption products.

In each location, the population size N_g is divided between workers L_g and non-workers $N_g - L_g$. Each of the two consumer types has, in principle, a distinct budget constraint, because income may differ depending on whether they work or not. However, we assume that workers pay lump-sum unemployment insurance (t_g) at the location where they provide labor services, and these taxes are fully redistributed as unemployment benefits (s_g) to the non-working individuals at the local level, that is, $t_g L_g = s_g (N_g - L_g)$. Furthermore, this redistribution is such that their incomes are equalized, $w_g - t_g = s_g$; where w_g is the wage rate. Which implies that $t_g = (N_g - L_g)w_g/N_g$ and then $w_g - t_g = L_g w_g/N_g$. That is, if there are more individuals unemployed, income per capita falls; and the opposite occurs if more people work. We also consider that consumers may pay lump-sum taxes τ_g that are directed to provide subsidies to firms. Therefore, letting l_g be the fraction of workers in region g (i.e., $l_g = L_g/N_g$), the budget constraint—which is the same for all consumers—can be written as:

$$l_g w_g + \frac{F_g + \tilde{D}_g}{N_g} - \tau_g = \sum_{j=1}^J \int_0^1 P_g^j(\Omega^j) c_g^j(\Omega^j) d\Omega^j; \quad (5a)$$

where $P_g^j(\Omega^j)$ is the price of variety Ω^j from sector- j consumed in g . The government of region g can also collect revenues from tariffs (F_g) that are redistributed to the whole local population. The term \tilde{D}_g represents the regional trade deficit. Financing a trade deficit requires the inflow of resources

⁴The assumption of a unitary elasticity of substitution in consumption might seem restrictive at first. However, it is worth pointing out that consumption in our framework denotes consumption of gross output, that is, final consumption expenditure. Herrendorf, Rogerson, and Valentinyi (2013) estimate an elasticity of substitution in the range of 0.85–0.89 but also show that an elasticity of 1 can fit aggregate consumption shares as good as a CES. As the number of sector increases, our assumption of a unitary elasticity becomes more credible.

from other locations, and this is why \tilde{D}_g appears in the consumer's budget constrain. Notice as well that this variable can be used in the experiments as a fiscal policy tool.

Given these preferences, the optimality conditions imply that the share of variety Ω^j in consumption expenditure on the goods produced by industry j is a function of relative prices and the elasticity of substitution. In particular,

$$\frac{P_g^j(\Omega^j)c_g^j(\Omega^j)}{P_g^j c_g^j} = \left[\frac{P_g^j(\Omega^j)}{P_g^j} \right]^{1-\varsigma^j}; \quad (6)$$

where P_g^j represents the ideal price index of the sector- j final products, which equals

$$P_g^j = \left[\int_0^1 P_g^j(\Omega^j)^{1-\varsigma^j} d\Omega^j \right]^{1/(1-\varsigma^j)}. \quad (7)$$

They also confirm that consumption expenditure on sector j products in a location g is a constant fraction of total income given by α_g^j .

Taking into account that budget constraint (5a) says that income is fully spent in buying consumption goods, we can write welfare, equation (3), using an indirect utility function approach as:

$$W_g = \frac{y_g}{P_g}; \quad (8)$$

where y_g is income per capita in region g , which equals

$$y_g = l_g w_g + \frac{F_g + \tilde{D}_g}{N_g} - \tau_g; \quad (9)$$

and P_g provides the ideal consumption price index that households face in location g ,

$$P_g = \prod_{j=1}^J \left(\frac{P_g^j}{\alpha_g^j} \right)^{\alpha_g^j}. \quad (10)$$

Note that welfare depends on the fraction of workers l_g and on the per-capita trade deficit and tariff revenue. Thus, shocks to a sector affect welfare through the trade deficit, the tariff revenues and the price index. Furthermore, constraining the share of working individuals in a region has *ceteris paribus* first order effects on welfare.⁵

⁵ In order to derive (8), notice that the indirect utility functions for working (W_g^L) and non-working (W_g^{NL}) individuals are, respectively,

$$W_g^L = \frac{1}{P_g} \left(w_g - t_g + \frac{F_g + \tilde{D}_g}{N_g} - \tau_g \right) \text{ and } W_g^{NL} = \frac{1}{P_g} \left(s_m + \frac{F_g + \tilde{D}_g}{N_g} - \tau_g \right).$$

Defining $N_g W_g = L_g W_g^L + (N_g - L_g) W_g^{NL}$ as total welfare in a location, W_g is given by

$$W_g = \frac{L_g}{N_g} W_g^L + \left(1 - \frac{L_g}{N_g} \right) W_g^{NL},$$

which, substituting each of the indirect utility functions, and recalling that $s_m = w_g - t_g = w_g L_g / N_g$ and that l_g represents the fraction of working individuals in a location g , we get equation (8)

3.1.2 Firms

In each location g , a firm that operates in sector j produces either an intermediate-good variety ($q_g^j(\omega^j)$, $\omega^j \in (0, 1)$), a final-product variety ($Q_g^j(\Omega^j)$, $\Omega^j \in (0, 1)$), or a composite intermediate or material ($Q_g^{\mathcal{M}j}$). The production of intermediate goods uses labor and materials from other industries, whereas the production process of final goods and materials demand intra-industry intermediates. Intermediate-good manufacturers and final-good and material producers in sector j may benefit from subsidization rates s_g^j and \mathfrak{s}_g^j , respectively, which reduce the costs of the different production inputs in the same proportion. All markets are perfectly competitive and firms maximize profits. We next describe in more detail each of the different stages of the production chain.

3.1.3 Intermediate goods

A firm in sector j produces a variety ω^j of intermediate goods using labor ($L_g^j(\omega^j)$) and composite intermediates from every other sector k ($m_g^{kj}(\omega^j)$) according to the production function:

$$q_g^j(\omega^j) = a_g^j z_g^j(\omega^j) L_g^j(\omega^j)^{\gamma_g^j} \prod_{k=1}^J m_g^{kj}(\omega^j)^{\gamma_g^{kj}}; \quad (11)$$

where a_g^j is sector j 's fundamental productivity in intermediate-goods manufacturing by region g ; $z_g^j(\omega^j)$ is a random sector-variety-specific productivity shock; and γ_g^j denotes the share of value added on gross output. The term affected by the product operator provides the use of materials from all other sectors, with γ_g^{kj} representing the expenditure share of the material from sector k employed in the input composite of the intermediate good produced by industry j . We assume that $\sum_{k=1}^J \gamma_g^{kj} = 1 - \gamma_g^j$. Production functions, then, exhibit constant returns to scale.

Because markets are perfectly competitive and firms are profit maximizers, intermediate-good prices must equal marginal costs, $b_g^j / [a_g^j z_g^j(\omega^j)]$; where b_g^j gives the cost of a unitary input bundle once subsidies are taken into account. The cost b_g^j is common to all varieties and given by

$$b_g^j = (1 - s_g^j) \Upsilon_g^j w_g^{\gamma_g^j} \prod_{k=1}^J (P_g^{\mathcal{M}k})^{\gamma_g^{kj}}; \quad (12)$$

where the constant Υ_g^j equals

$$\Upsilon_g^j = \left(\frac{1}{\gamma_g^j} \right)^{\gamma_g^j} \prod_{k=1}^J (\gamma_g^{kj})^{-\gamma_g^{kj}};$$

$P_g^{\mathcal{M}k}$ is the price of the composite intermediate produced by sector k in region g ; and w_g denotes the wage rate in location g . Equation (12) says that the subsidy will translate into lower prices because it complements market revenues at paying for the inputs. Notice that the term $1 - s_g^j$ can be written as a common factor because of constant returns to scale and because production subsidies reduce all input costs by the same proportion.

3.1.4 Final products

In each sector-region (j, g) pair, a set of final goods indexed by Ω^j are produced under perfect competition using intermediate goods from the same sector following a Dixit-Stiglitz aggregator with a constant elasticity of substitution $\sigma^j > 1$:

$$Q_g^j(\Omega^j) = A_g^j Z_g^j(\Omega^j) \left[\int_0^1 r_g^j(\omega^j)^{1-1/\sigma^j} d\omega^j \right]^{\frac{\sigma^j}{\sigma^j-1}}; \quad (13)$$

where A_g^j is the sector-region fundamental productivity in final-goods production; $r_g^j(\omega^j)$ represents the demand in region g for intermediate good ω^j from the lowest-cost supplier, which can belong to any of the regions.

Profit maximization implies the following demand function for each of the varieties:

$$r_g^j(\omega^j) = \left[\frac{(1 - \mathfrak{s}_g^j) p_g^j(\omega^j)}{B_g^j} \right]^{-\sigma^j} \frac{Q_g^j(\Omega^j)}{A_g^j Z_g^j(\Omega^j)}; \quad (14)$$

where $p_g^j(\omega^j)$ is the price of intermediate good ω^j in location g ; and B_g^j gives the cost of the input bundle with subsidies already embedded as

$$B_g^j = (1 - \mathfrak{s}_g^j) \left[\int_0^1 p_g^j(\omega^j)^{1-\sigma^j} d\omega^j \right]^{\frac{1}{1-\sigma^j}}. \quad (15)$$

Equation (14) implies that the demand of intermediate ω^j per unit of final output depends on the ω^j 's price relative to the price of the other varieties of intermediates. Consequently, as a response to the subsidy, the amount for intermediate products demanded can increase, not because of a change in the price that firms perceived $((1 - \mathfrak{s}_g^j) p_g^j(\omega^j))$, but because of the decrease in the price of the final output (given by the marginal cost), which can cause an increase in $Q_g^j(\Omega^j)$.

3.1.5 Composite intermediate goods

Production of materials in sector j uses a very similar technology to the one of final goods. In particular,

$$Q_g^{\mathcal{M}j} = A_g^j \left[\int_0^1 r_g^j(\omega^j)^{1-1/\sigma^j} d\omega^j \right]^{\frac{\sigma^j}{\sigma^j-1}}. \quad (16)$$

That is, it also combines varieties of intermediate goods coming from the same sector. The difference with equation (13) is that productivity in the case of the production of the composite intermediate is fully deterministic. Clearly, the demand for intermediate inputs will be very similar to the one delivered by final goods; in particular,

$$r_g^j(\omega^j) = \left[\frac{(1 - \mathfrak{s}_g^j) p_g^j(\omega^j)}{B_g^j} \right]^{-\sigma^j} \frac{Q_g^{\mathcal{M}j}}{A_g^j}; \quad (17)$$

Because composite intermediate goods do not engage in inter-regional trade, the price paid for them by intermediate-goods manufacturers is directly given by the marginal cost of production in the

same location. This implies that

$$P_g^{\mathcal{M}j} = \frac{B_g^j}{A_g^j}. \quad (18)$$

3.1.6 Inter-regional trade and destination prices

Intermediate goods and final products can travel across locations. Inter-regional trade is costly. Trade costs combine tariffs and iceberg transportations costs. We consider that tariff may be different for intermediate and final goods. More specifically, a sector- j intermediate imported by region g from location i involves a trade cost equal to

$$\kappa_{gi}^j = \left(1 + \tau_{gi}^j\right) d_{gi}^j; \quad (19)$$

where τ_{gi}^j is the imposed ad-valorem tariff on intermediate goods from sector j . The transportation cost d_{gi}^j implies that the arrival of one unit of an intermediate product to g coming from i requires sending d_{gi}^j units produced of that product. For the case of final goods, trade costs equal

$$K_{gi}^j = \left(1 + T_{gi}^j\right) \mathfrak{d}_{gi}^j. \quad (20)$$

Now T_{gi}^j represents the tariff on final goods from industry j , and \mathfrak{d}_{gi}^j the iceberg costs related to trade in final goods. Because we will use changes in iceberg costs as proxies to study the effect of supply-chain disruptions, it is only assumed that $d_{gi}^j, \mathfrak{d}_{gi}^j \geq 1$ for all g and i . For the same reason, the usual triangular inequality $\kappa_{gi}^j \leq \kappa_{hi}^j \kappa_{gh}^j$ and $K_{gi}^j \leq K_{hi}^j K_{gh}^j$ may not hold for all g, i and h .

Taking into account these trade costs, the prices at destination of the traded products from the lowest-cost supplier are the following:

$$p_g^j(\omega^j) = \min_{i \in [1, G]} \left\{ \frac{b_i^j \kappa_{gi}^j}{a_g^j z_g^j(\omega^j)} \right\} \quad (21)$$

and

$$P_g^j(\Omega^j) = \min_{i \in [1, G]} \left\{ \frac{B_i^j K_{gi}^j}{A_g^j Z_g^j(\Omega^j)} \right\}. \quad (22)$$

Equations (21) and (22) say that the price at destination will be given by the minimum across locations of the product between the marginal cost and the trade cost. A more expensive input bundle or higher trade costs will push the price up, whereas a larger productivity will push it down.

Following Eaton and Kortum (2002), trade in the model obeys a Ricardian motive generated by a random allocation of productivities across sectors and regions. In particular, the realizations of the productivity variables z_g^j and Z_g^j for varieties ω^j and Ω^j follow Fréchet distributions with location parameter equal to *one* and sector-specific shape parameters θ^j and Θ^j , respectively. A smaller value of the shape parameter implies a larger dispersion of the distribution. We suppose that the random productivity variables are independently distributed across goods, industries and regions, and that

$1 + \theta^j > \sigma^j$ and $1 + \Theta^j > \varsigma^j$. Results in Caliendo and Parro (2015) imply that, with these assumptions on the distribution of efficiencies, the distribution of prices allow rewriting equations (15) and (7) as

$$B_g^j = (1 - \mathfrak{s}_g^j) \Gamma \left(1 + \frac{1 - \sigma^j}{\theta^j} \right)^{1/(1 - \sigma^j)} \left[\sum_{i=1}^G \left(\frac{b_i^j \kappa_{gi}^j}{a_i^j} \right)^{-\theta^j} \right]^{-1/\theta^j}, \quad (23)$$

$$P_g^j = \Gamma \left(1 + \frac{1 - \varsigma^j}{\Theta^j} \right)^{1/(1 - \varsigma^j)} \left[\sum_{i=1}^G \left(\frac{B_i^j K_{gi}^j}{A_i^j} \right)^{-\Theta^j} \right]^{-1/\Theta^j}; \quad (24)$$

where $\Gamma(\cdot)$ is the gamma function.

In the case that a sector is not tradable, which implies that all the varieties of intermediate goods and consumption products from that sector are bought from domestic producers, Caliendo and Parro (2015) also show that the relevant price indices amount to imposing that $\kappa_{gi}^j = K_{gi}^j = \infty$ for all $i \neq g$ in equations (23) and (24). Then, we end up with $B_g^j = (1 - \mathfrak{s}_g^j) \Gamma(1 + (1 - \sigma^j)/\theta^j)^{1/(1 - \sigma^j)} b_g^j/a_g^j$ and $P_g^j = \Gamma(1 + (1 - \varsigma^j)/\Theta^j)^{1/(1 - \varsigma^j)} B_g^j/A_g^j$.

3.1.7 Expenditure Shares

Let x_g^j and X_g^j be region g 's total expenditures on intermediate goods and final products from sector j , respectively. They are obtained at destination prices, and therefore, include tariff payments. Define x_{gi}^j and X_{gi}^j as the expenditures in location g on sector- j intermediate goods and sector- j final products, respectively, imported by location g from location i . Finally, let π_{gi}^j and Π_{gi}^j be region g 's total expenditure shares of intermediate goods and final products from sector j exported by location i to location g , respectively; that is, $\pi_{gi}^j = x_{gi}^j/x_g^j$ and $\Pi_{gi}^j = X_{gi}^j/X_g^j$. Caliendo and Parro (2015) show that

$$\pi_{gi}^j = \frac{\left(b_i^j \kappa_{gi}^j / a_i^j \right)^{-\theta^j}}{\sum_{h=1}^G \left(b_h^j \kappa_{gh}^j / a_h^j \right)^{-\theta^j}}, \quad (25)$$

$$\Pi_{gi}^j = \frac{\left(B_i^j K_{gi}^j / A_i^j \right)^{-\Theta^j}}{\sum_{h=1}^G \left(B_h^j K_{gh}^j / A_h^j \right)^{-\Theta^j}}. \quad (26)$$

Bilateral trade shares contain important information. First, they are declining on transport costs and increasing in the productivity of the producer (since this productivity reduces the marginal cost directly). Second, they include information on the input-output structure of the whole economy through the prices paid for intermediate inputs. Furthermore, this input-output structure is also affected by the economic geography, since intermediate inputs can be imported from abroad. In terms of the effects of policies regarding the control of COVID-19, this gravity equation is potentially informative for several reasons. It can potentially capture the fact that some sectors might be more

affected by social distancing policies, since sectors can differ in their labor input intensities. [Dingel and Neiman \(2020\)](#) estimate that, in the U.S., the share of jobs that can be done from home significantly varies across cities and industries and also show that this share is decreasing in the level of development of the countries. Our model could plausibly capture this. Our model could also show the effects of how shutting down a certain sector or region, would affect the rest of sectors and locations through the input-output structure. Furthermore, in the second phase of the model, infections can be spread through economic linkages, since some sectors are more interconnected than others, those regions that are more intensive in certain inputs can show significantly faster infection rates.

3.1.8 Market clearing and government and regional deficits

Local labor markets require that the sum of labor employed in the different industries equals the total amount of labor available in the region. Formally,

$$\sum_{j=1}^J L_g^j = L_g \quad (27)$$

Furthermore, because in equilibrium labor costs must equal a constant fraction γ_g^j of the value of the intermediate-goods production, the following condition must hold:

$$w_g L_g = \sum_{j=1}^J \frac{\gamma_g^j}{1 - s_g^j} \sum_{i=1}^G \frac{x_i^j \pi_{ig}^j}{1 + \tau_{ig}^j}. \quad (28)$$

Notice that the right hand side (RHS) of equation (28) adds the expenditures across sectors and regions on intermediate goods manufactured in location g that go to pay the labor input. It also implies that payments to labor are in part satisfied using the subsidies, in an amount equivalent to a fraction $\gamma_g^j s_g^j / (1 - s_g^j)$ of the revenues from sales. We divide by the tariff to convert each expenditure amount into the value of production.

In the same manner, the total value of the production of composite intermediates from sector j in a location g has to be equal to a subsidy-weighted fraction (determined by the γ_g^{jk} s) of the expenditure on region g 's intermediate goods across sectors and locations. In particular,

$$P_g^{\mathcal{M}j} Q_g^{\mathcal{M}j} = \sum_{k=1}^J \frac{\gamma_g^{jk}}{1 - s_g^j} \sum_{i=1}^G \frac{x_i^k \pi_{ig}^k}{1 + \tau_{ig}^k}. \quad (29)$$

Notice that market clearing conditions (28) and (29) imply as well that the intermediate goods market clears.

Employing again a production-expenditure equality, market clearing in the location g 's final-goods market requires that the value of the sector- j final-goods produced in g equals the consumption expenditure across regions on final products from that location. Taking into account that the revenues from the production activity of the final-product sector fully goes to pay for the intermediate goods

used as inputs, we can write the market clearing condition as:

$$x_g^j - \frac{P_g^{\mathcal{M}j} Q_g^{\mathcal{M}j}}{1 - \mathfrak{s}_g^k} = \frac{1}{1 - \mathfrak{s}_g^k} \sum_{i=1}^G \frac{X_i^j \Pi_{ig}^j}{1 + T_{ig}^j}. \quad (30)$$

The left hand side of equation (30) subtracts the value of materials to provide just the amount of expenditure in intermediate goods satisfied by final-goods producers. The subsidy \mathfrak{s}_g^k is in the equation because the expenditure on inputs, x_g^j , equals the market revenues—given by the terms affected by the sum operator—plus the subsidies received by the industry.

Note that consumers' expenditure on sector- j products in region- i is a fixed fraction α_i^j of their income. Hence,

$$X_i^j = \alpha_i^j y_i N_i; \quad (31)$$

where income per capita y_i , given by equation (9), is a function of tariff revenues. We can now write those revenues using the notation introduced previously as:

$$F_g = \sum_{j=1}^J \sum_{i=1}^G \left(\tau_{gi}^j \frac{x_g^j \pi_{gi}^j}{1 + \tau_{gi}^j} + T_{gi}^j \frac{X_g^j \Pi_{gi}^j}{1 + T_{gi}^j} \right). \quad (32)$$

Moving next to the determination of the trade balance, we consider that the regional trade deficit \tilde{D}_g is given by the sum of the sectoral deficits, \tilde{D}_g^j . The sectoral deficit \tilde{D}_g^j equals the value of the region g 's imports of industry- j goods from all other locations minus the value of exports of sector- j products from location g to all other locations. This is equivalent to imposing that the deficit is given by the difference between total expenditure by region g on sector- j intermediate and final products net of tariffs and the total value of production of industry- j intermediate and final goods in location g . More specifically,

$$\tilde{D}_g^j = \sum_{i=1}^G \left(\frac{x_g^j \pi_{gi}^j}{1 + \tau_{gi}^j} + \frac{X_g^j \Pi_{gi}^j}{1 + T_{gi}^j} \right) - \sum_{i=1}^G \left(\frac{x_i^j \pi_{ig}^j}{1 + \tau_{ig}^j} + \frac{X_i^j \Pi_{ig}^j}{1 + T_{ig}^j} \right). \quad (33)$$

The second parenthesis gives the value of production by adding across locations the amount spent on products from the sector-region pair (j, g) net of tariffs.

Therefore, trade balance in location g implies the the sum of the sectoral trade deficits must equal the regional one, which means

$$\tilde{D}_g = \sum_{j=1}^J \tilde{D}_g^j. \quad (34)$$

It can be shown that the trade balance condition, equation (34) implies that the labor market clears, that is, equation (28).

Finally, we allow for the possibility that the regional budget deficit, denoted by \bar{D}_g , is not zero. Therefore, the following condition must hold:

$$\bar{D}_g = \sum_{j=1}^J \sum_{i=1}^G \left(\frac{s_g^j}{1 - s_g^j} \frac{x_i^j \pi_{ig}^j}{1 + \tau_{ig}^j} + \frac{\mathfrak{s}_g^j}{1 - \mathfrak{s}_g^j} \frac{X_i^j \Pi_{ig}^j}{1 + T_{ig}^j} \right) + \sum_{j=1}^J \frac{\mathfrak{s}_g^j}{1 - \mathfrak{s}_g^j} P_g^{\mathcal{M}j} Q_g^{\mathcal{M}j} - \tau_g N_g. \quad (35)$$

That is, if the expenditure in subsidies is larger than the taxes collected to finance them, there will be a positive budget deficit.

3.1.9 Equilibrium system in relative changes

As in [Caliendo and Parro \(2014\)](#), we solve the model in changes. Let us denote a proportional change in a variable with a hat ($\hat{\cdot}$) and the value of the variable next period with a prime ($'$). Then, for example, $\hat{\tau}_{gi}^j = \tau_{gi}^{j'}/\tau_{gi}^j$. The exogenous shocks that we will consider correspond to new tariffs, $\tau_{gi}^{j'}$ and $T_{gi}^{j'}$, new subsidies to firms, $s_g^{j'}$ and $\mathfrak{s}_g^{j'}$, supply-chain disruptions proxied by changes in the trade costs, \hat{d}_{gi}^j and $\hat{\mathfrak{d}}_{gi}^j$ for $g \neq i$, local production restrictions proxied by \hat{d}_{gg}^j and $\hat{\mathfrak{d}}_{gg}^j$, and confinement policies captured by new stocks of available labor in the region, L_g' .

Equations (12) and (18) imply that the gross growth rate in the cost of the intermediate-goods input bundle equals

$$\hat{b}_g^j = \left(\frac{1 - s_g^{j'}}{1 - s_g^j} \right) \hat{w}_g^{\gamma_g^j} \prod_{k=1}^J \left(\hat{B}_g^k \right)^{\gamma_g^{kj}}. \quad (36)$$

In turn, combining expressions (23) and (25) obtains the change in the cost of the final-goods input bundle and the export shares of intermediate products as

$$\hat{B}_g^j = \left(\frac{1 - \mathfrak{s}_g^{j'}}{1 - \mathfrak{s}_g^j} \right) \left[\sum_{i=1}^G \pi_{gi}^j \left(\hat{b}_i^j \hat{\kappa}_{gi}^j \right)^{-\theta^j} \right]^{-1/\theta^j} \quad (37)$$

and

$$\hat{\pi}_{gi}^j = \left(\frac{\hat{b}_i^j \hat{\kappa}_{gi}^j}{\hat{B}_g^j} \right)^{-\theta^j}, \quad (38)$$

respectively; where $\hat{\kappa}_{gi}^j = (1 + \tau_{gi}^{j'}) \hat{d}_{gi}^j / (1 + \tau_{gi}^j)$. The gross growth rate in the sectoral price index and the final-good export shares are delivered by equations (24) and (26) as

$$\hat{P}_g^j = \left[\sum_{i=1}^G \Pi_{gi}^j \left(\hat{B}_i^j \hat{K}_{gi}^j \right)^{-\Theta^j} \right]^{-1/\Theta^j} \quad (39)$$

and

$$\hat{\Pi}_{gi}^j = \left(\frac{\hat{B}_i^j \hat{K}_{gi}^j}{\hat{P}_g^j} \right)^{-\Theta^j}, \quad (40)$$

respectively; where $\hat{K}_{gi}^j = (1 + T_{gi}^{j'}) \hat{\mathfrak{d}}_{gi}^j / (1 + T_{gi}^j)$.

Market clearing conditions can be employed to obtain the future values of the expenditure variables as a function of the above changes. In particular, market clearing for final-goods, equations (29) and (30), implies that region g 's next-period expenditure in intermediate goods from sector j is given by:

$$x_g^{j'} = \frac{1}{1 - \mathfrak{s}_g^{j'}} \left(\sum_{k=1}^J \sum_{i=1}^G \frac{\gamma_g^{jk}}{1 - s_g^{j'}} \frac{x_i^{k'} \pi_{ig}^{k'}}{1 + \tau_{ig}^{k'}} + \sum_{i=1}^G X_i^{j'} \frac{\Pi_{ig}^{j'}}{1 + T_{ig}^{j'}} \right). \quad (41)$$

Notice that $\pi_{ig}^{k'}$ and $\Pi_{ig}^{j'}$ can be written as $\pi_{ig}^k \hat{\pi}_{ig}^k$ and $\Pi_{ig}^j \hat{\Pi}_{ig}^j$, respectively.

From equations (9), (29), (31), (32) and (35), next-period's expenditure in final goods from sector j equals:

$$X_g^{j'} = \alpha_g^j \left[L_g' w_g' + \sum_{k=1}^J \sum_{i=1}^G \left(\tau_{gi}^{k'} \frac{x_g^{k'} \pi_{gi}^{k'}}{1 + \tau_{gi}^{k'}} + T_{gi}^{k'} \frac{X_g^{k'} \Pi_{gi}^{k'}}{1 + T_{gi}^{k'}} \right) + \tilde{D}_g' - \tau_g' N_g \right]; \quad (42)$$

where

$$\tilde{D}_g' = \sum_{j=1}^J \sum_{i=1}^G \left(\frac{x_g^{j'} \pi_{gi}^{j'}}{1 + \tau_{gi}^{j'}} + \frac{X_g^{j'} \Pi_{gi}^{j'}}{1 + T_{gi}^{j'}} \right) - \sum_{j=1}^J \sum_{i=1}^G \left(\frac{x_i^{j'} \pi_{ig}^{j'}}{1 + \tau_{ig}^{j'}} + \frac{X_i^{j'} \Pi_{ig}^{j'}}{1 + T_{ig}^{j'}} \right). \quad (43)$$

Again, we can write w_g' as $w_g \hat{w}_g$ so that it becomes a function of the changes determined by previous equations in the system.

The system formed by equations (36) to (43) is underdetermined because the number of unknowns is equal to the number of equations plus one. In order to solve it, [Caliendo and Parro \(2014\)](#) assume that the economy's trade deficit in each location g is exogenous. We, on the other hand, allow for the trade deficit to be determined by the model and, instead, required that the wage rate does not vary. This looks to us more appropriate for the problem that we analyze.

Equations (36) to (43) imply that we do not need to calibrate fundamental productivities and trade costs to solve the system. We simply start from a baseline scenario that consists of initial data on regional wages, labor, and trade and budget deficits $\{w_g, L_g, \tilde{D}_g, \bar{D}_g\}_{g=1}^G$, pairwise regional expenditure shares and tariffs in every sector $\{\pi_{gi}^j, \Pi_{gi}^j, \tau_{gi}^j, T_{gi}^j\}_{g=1, i=1, j=1}^{G, G, J}$, and the assumption of no subsidies for firms, $s_g^j = \mathfrak{s}_g^j = 0$. We also need to assign values to the labor share in gross output (γ_g^j), the share of intermediate goods from sector k employed in the production of sector j (γ_g^{jk}), the share of consumption expenditure on sector- j goods (α_g^j), and the shape parameters θ^j and Θ^j of the Fréchet distributions. With that information on our hands, we consider shocks on the values τ_{gi}' , T_{gi}' , $s_g^{j'}$, $\mathfrak{s}_g^{j'}$, \hat{d}_{gi}^j , $\hat{\mathfrak{d}}_{gi}^j$ and/or L_g' , and solve the system going through the following steps.

1. Assume $\hat{w}_g = 0$ for all g .
2. From equations (36) and (37) obtain $\{\hat{b}_g^j, \hat{B}_g^j\}_{g=1, j=1}^{G, J}$.
3. Once we know the cost of the unitary input bundles, we recover the values of $\{\hat{P}_g^j, \hat{\pi}_{gi}^j, \hat{\Pi}_{gi}^j\}_{g=1, i=1, j=1}^{G, G, J}$ from equations (39) to (40).
4. Obtain $\{x_g^{j'}, X_g^{j'}\}_{g=1, j=1}^{G, J}$ using (41) and (42).

The above implies that, in this economy, an equilibrium in relative changes can be defined as follows. Given the new value of the regional labor supply $\{L_g\}_{g=1}^G$, regional deficits $\{\tilde{D}_g, \bar{D}_g\}_{g=1}^G$, and pairwise regional government policies in every industry $\{\tau_{gi}^{j'}, T_{gi}^{j'}\}_{g=1, i=1, j=1}^{G, G, J}$, a competitive equilibrium is a set of changes in intermediate-good and final-product price indices in for each sector-location pair $\{\hat{B}_g^j, \hat{P}_g^j\}_{g=1, j=1}^{G, J}$, and pairwise regional expenditure shares in every sector $\{\hat{\pi}_{gi}^j, \hat{\Pi}_{gi}^j\}_{g=1, i=1, j=1}^{G, G, J}$, in addition to new values of the total sector-location expenditure volumes $\{x_g^{j'}, X_g^{j'}\}_{g=1, j=1}^{G, J}$, such

that the optimizing conditions for households, intermediate-product manufacturers, final-good firms and material producers—which are reflected in equations (12), (18), (23) to (26) and (31)—hold, and market clearing in all markets is achieved through conditions (29), (30) and (33).

3.2 Phase 2: Infection Dynamics

The dynamics take place at the *local* level but we allow for possible contagions across locations depending on effective distance. Typically, epidemiology models characterize the transitions from one state to another with exogenously given probabilities that refer to the characteristics of the particular infection. Here, instead, we assume that transition probabilities depend on two factors, one exogenous that captures the characteristics of the infection, and an endogenous geographic component that captures how more economically active locations can be more prone to infections since they have more connections with the rest of locations.

People that work face-to-face, people that work telematically, and people that do not work have different probabilities of catching the disease due to their different number of encounters with other people. Additionally, individuals that have recovered from the disease or have been vaccinated can have a lower probability of becoming infected. We assume that all the infected, regardless of whether they are in hospital or not, are able to pass the disease to workers; obviously, if the infected is in a hospital, they can pass the disease mainly to health workers.

We consider two scenarios where people can become infected. First, infections occur *locally* through social interactions not related to market activities, like for example visiting relatives at home or walking in the streets. Second, the virus can be transmitted through a *market related* activity, what we call the *geographic component*, such as workers producing output, consumers enjoying a beverage in a cafeteria, or product trade. Within this second component, the movement of goods and services within and between regions can also be an important vector for the transmission of the disease, because some degree of human interaction is needed to arrange those transactions. For example, when infected people buy tourism or via infected truck drivers. Actually, Oster (2012) finds that doubling exports increases HIV infections by 10-70% through truckers in Africa. Importantly, truck transportation is responsible for the movement of 80% of the world's goods. In the same vein, Adda (2016) finds that the expansion of transportation networks and inter-regional trade explains an important part of the prevalence of infection diseases in France.

Locally, susceptible individuals get infected with probability denoted by $(1-\kappa)\rho_g$; where κ captures the proportion of infections that arise in market-related contexts (trade or production) and is time-invariant. The time-varying probability ρ_g provides the likelihood that a susceptible individual gets the disease if an infected agent is met. The parameter ρ_g is affected by local policies, local behaviors, and other non-production related characteristics. The weight of the geographic component, in turn,

depends on the level of market activity. This can be captured by the expenditure variables x_{ig}^j and X_{ig}^j . Hence, the dynamics for infected people can be written as:

$$I'_g = \underbrace{(1 - \varphi)I_g}_{\text{Infected not becoming resolving}} + S_g \Phi_g; \quad (44)$$

where the term Φ_g is given by

$$\Phi_g = \underbrace{(1 - \kappa)\rho_g \frac{I_g}{N_g}}_{\text{Local Component}} + \underbrace{\kappa \left(\sum_{i=1}^G \rho_i \frac{I_i}{N_i} \Lambda_i \tilde{X}_{ig} \right)}_{\text{Geographic Component}}; \quad (45)$$

and the coefficient φ gives the fraction of infected that become resolving every period.

According to motion equation (44), the number of infected people tomorrow depends on infected people today net of those that become resolving cases. The equation also considers that the susceptible can catch the disease. As expression (45) specifies, this can occur through the local and the geographic components. The strength of the latter depends on the contagion probability and the prevalence of the disease in the trade partner and also on the relative level of human interactions in transactions. In particular, the term \tilde{X}_{ig} represents the level of market interaction between any two regions i and g , and is given by:

$$\tilde{X}_{ig} = \frac{\sum_{j=1}^J (x_{ig}^j + x_{gi}^j + X_{ig}^j + X_{gi}^j)}{\sum_{h=1}^G \sum_{k=1}^J (x_{hg}^k + x_{gh}^k + X_{hg}^k + X_{gh}^k)} \quad (46)$$

It says that the human-interaction level between two economies i and g is a function of bilateral imports and exports if two different locations are involved or a function the local expenditure volumes if market activity is fully local. Notice that the bilateral trade volumes in equation (45) are weighted by a region variable Λ_i that controls for the degree of telematic work, among other things.⁶

The following equations, along with equation (44), describe the full epidemiological model:

$$S'_g = (1 - \lambda_g - \Phi_g)S_g + \alpha^V V_g + \alpha^C C_g \quad (47a)$$

$$V'_g = (1 - \alpha^V)V_g + \lambda_g S_g \quad (47b)$$

$$R'_g = \varphi I_g + (1 - \xi)R_g \quad (47c)$$

$$C'_g = (1 - \alpha^C)C_g + (1 - \delta)\xi R_g \quad (47d)$$

$$F'_g = F_g + \delta\xi R_g \quad (47e)$$

$$N'_g = N_g - \delta\xi R_g \quad (47f)$$

The parameter λ_g represents the fraction of the susceptible that are vaccinated during the period in location g ; α_c and α_v are the fraction of the recovered and the vaccinated that fully lose immunity,

⁶It can be show that the basic reproduction number of the disease, \mathcal{R}_0 , increases in our setup with the level of trade integration between two regions, \tilde{X}_{ig} . See appendix A for the details. The coefficient \mathcal{R}_0 represents the average number of secondary infections produced by a typical case of an infection in a population where everyone is susceptible.

respectively; the parameter ξ reflects the fraction of cases that resolve in a given period, and therefore, its inverse pins down the average number of periods it takes for a case to resolve; and φ relates to the average number of days ($1/\varphi$) a person is infectious.

Equation (47a) says that the size of the susceptible population decreases with the fraction λ_g that receives the vaccine and the fraction Φ_g that gets infected by the Covid-19 virus, but rises with the recovered and vaccinated that lose their immunity. The vaccinated population, equation (47b), increases with the fraction of the susceptible that receive the vaccine and decreases with the vaccinated individuals that lose immunity. In equation (52), in turn, a fraction φ of infected individuals become resolving, and a fraction ξ of cases are resolved. The number of recovered individuals, equation (47d), evolves in a similar way as the one of the vaccinated: a fraction α_c lose their immunity and some of the resolving, among the fraction δ that survives, recover during the period. The evolution of the stock of fatalities (F_g) is simple, (47e) implies that the new deaths come from the fraction ($\delta\xi$) of resolving that resolve and die. Finally, the evolution of the region's population is given by equation (47f), which implies that a fraction $\delta\xi$ of the resolving cases die.

4 Calibration

The main source for the calibration of the economic part of the model is [Thiessen \(2020\)](#), which offers the Rhomolo-MRIO Tables for 2013 published by the European commission. The dataset provides input-output tables for a set of 268 regions that include 267 EU28 NUTS2-2010 areas plus the rest of the world (ROW). Nevertheless, due to the lack of sufficiently disaggregated data for the disease variables, we need to aggregate some locations to the NUTS1 and country levels. After doing so, we are left with 230 regions (see Table 1). The numbers are disaggregated into ten main sectors of activity belonging to the NACE Rev2 classification (see Table 2). A summary of the data sources employed for the calibration of both the economic and disease parameters—and sometimes their values—are provided in Table 3.

From [Thiessen \(2020\)](#), we also compute α_g^j , that is, the shares of the different sectors in total consumption expenditure in each location. The same dataset allows deriving estimates of the share of value added on gross output, γ_g^j , and the expenditure share of each material employed in the input composite of the intermediate good produced by other industries, γ_g^{kj} .⁷

The sector-specific shape parameters θ^j and Θ^j of the Fréchet distributions related to the productivity variables z_g^j and Z_g^j , respectively, are obtained as follows. Consider two regions, i and g , and the bilateral trade expenditures between the two, x_{gi}^j , x_{ig}^j , X_{gi}^j and X_{ig}^j . Recall that expenditure shares $\pi_{gi}^j = x_{gi}^j/x_g^j$ and $\Pi_{gi}^j = X_{gi}^j/X_g^j$ are given in equilibrium by equations (25) and (26). These

⁷Due to the large number of observations, these and other parameter and variable values are not reported in the paper. They are available from the authors upon request.

expressions imply that we can write:

$$\frac{x_{gi}^j x_{ig}^j}{x_{gg}^j x_{ii}^j} = \left(\frac{\kappa_{gi}^j \kappa_{ig}^j}{\kappa_{gg}^j \kappa_{ii}^j} \right)^{-\theta^j}, \quad (48)$$

and

$$\frac{X_{gi}^j X_{ig}^j}{X_{gg}^j X_{ii}^j} = \left(\frac{K_{gi}^j K_{ig}^j}{K_{gg}^j K_{ii}^j} \right)^{-\theta^j}. \quad (49)$$

Equations (48) and (49) provide gravity equations for intermediate and final products, respectively. They present bilateral trade expenditures as a function of bilateral trade costs. Equations (19) and (20) say that trade costs are composed of tariffs and iceberg costs. We assume, for the only purpose of estimating the trade shares, that $d_{gi}^j = \mathfrak{d}_{gi}^j = v_{gi} e^{\mu_g^j + \eta_i^j + \varepsilon_{gi}^j}$; where $v_{gi} = v_{ig}$ represents symmetric bilateral trade costs like distance (geographical, language, etc...) or belonging to a certain trade agreement; μ_g^j and η_i^j capture sector-specific fixed effects in the importer and exporter regions, respectively; and ε_{gi}^j is a random disturbance. Substituting those expressions for trade costs into (48) and (49), equalizing tariffs to zero and taking logs, we obtain:

$$\ln \left(\frac{x_{gi}^j x_{ig}^j}{x_{gg}^j x_{ii}^j} \right) = -\theta^j \ln \left(\frac{v_{gi} v_{ig}}{v_{gg} v_{ii}} \right) + \tilde{\varepsilon}_{gi}^j;$$

and

$$\ln \left(\frac{X_{gi}^j X_{ig}^j}{X_{gg}^j X_{ii}^j} \right) = -\Theta^j \ln \left(\frac{v_{gi} v_{ig}}{v_{gg} v_{ii}} \right) + \tilde{\varepsilon}_{gi}^j;$$

where $\tilde{\varepsilon}_{gi}^j = \varepsilon_{gi}^j + \varepsilon_{ig}^j - \varepsilon_{gg}^j - \varepsilon_{ii}^j$. Hence, all asymmetric components of the iceberg costs (μ_g^j , μ_i^j , η_g^j and η_i^j) have cancelled out. In addition, we have equalized tariffs to zero because, in the estimation, we use data on export spending for the EU28 in 2013 from [Thiessen \(2020\)](#) but exclude the flows from and to the rest of the world; clearly, trade among EU members are not subject to tariffs or other trade restrictions.

As proxy for the symmetric component of the bilateral trade costs, we employ distance between regions obtained from [Persyn, Diaz-Lanchas, Barbero, Conte, and Salotti \(2019\)](#). This dataset gives estimates of different distance measures between EU regions at the NUTS2 level. We choose the distance measure that provides arithmetic averages over the geodesic distance between many centroids for each region-pair. Each region have more than one centroid and then $v_{gg} > 1$. In the estimation, we use data on expenditure variables (x_{gi}^j and X_{gi}^j) from the original 267 European regions considered in [Thiessen \(2020\)](#) to maximize the amount of information. The results of the estimation of the trade elasticities are presented in Table 4. The estimates range from 1.99 to 3.09 for intermediate goods and from 1.94 to 3.09 for final products. The smallest elasticity corresponds to construction (sector C), and the largest to public administration, defence, education, human health and social work activities (sectors O_Q).

We now turn to the parameters that govern the disease dynamics. We set the values for Λ_g from [Dingel and Neiman \(2020\)](#). In particular, we estimate the percentage of workers in each sector that can work from home ς_j and then, for each region, we compute Λ_g as

$$\Lambda_g = 1 - \sum_{j \in J} \varsigma_j \frac{x_g^j + X_g^j}{\sum_{k \in J} x_g^k + X_g^k}$$

which is a weighted average where the weights are sectoral expenditure shares. This takes into account the sectoral composition of each region.

Parameter κ comes from [Eichenbaum, Rebelo, and Trabandt \(2020\)](#) who estimate 17% of infections related to work environments. We take φ , ξ and δ from [Fernandez-Villaverde and Jones \(2020\)](#). The parameter φ is equalized to 0.125, which implies that an individual is infectious for 8 days, and ξ to 0.143 so that the average case takes 15 days to fully resolve (8 days infectious plus 7 of resolving). The mortality rate δ is taken which is set to 1%.

Next, since we focus on the first wave, we equalize to zero the vaccination rate λ_g and the immunization loss for vaccinated α^V . The evidence on reinfection rates for COVID-19 is still unclear. Regarding reinfection among those not vaccinated, [Sheehan, Reddy, and Rothberg \(2021\)](#) estimate that the protection from getting infected ranges from 81.8–84.5%. Taking into account this evidence, we fix $\alpha^C = 0.168$ which implies a protection from the infection of 83.15%.

Finally, we recover the time-variant ρ_g , that is, the probability that a susceptible individual gets the disease.⁸ Because some regions do not have data on Covid-19 daily deaths (see Table 5 for details), we need to split our sample in two groups. The first group is composed of those areas that do report daily deaths. The second one, in turn, is the set of regions that only report confirmed cases. For those regions that report deaths, we extend the approach suggested by [Fernandez-Villaverde and Jones \(2020\)](#), which essentially boils down to obtaining ρ_g as a residual using data on deaths only. This method is explained in detailed in appendix B.⁹

However, sometimes in a region, we encounter three consecutive days with zero deaths and the method breaks down. When this occurs, we estimate a constant infection rate $\bar{\rho}_g$ for the region that presents the problem as follows. We first make $\kappa = 0$ to eliminate the geographic component so that we can obtain a $\bar{\rho}_g$ in isolation from other regions. Then, we estimate $\bar{\rho}_g$ by NLLS so as to minimize the distance of the predicted deaths from the actual death observations. This estimated average infection rate is assigned ($\rho_g = \bar{\rho}_g$) only to the periods in which it is not possible to recover

⁸For the calibration of the remaining disease parameters and initial values, ROW was assumed to be composed by China, the U.S. and Switzerland. This means that for both, the EU27 and the UK, we consider at least 70% of the trade volumes with other areas.

⁹In the calibration of ρ_g , we eliminate the geographical component, that is, take $\kappa = 0$. The reason is that, in many periods, the large number of zero deaths makes the system where the $\{\rho_g\}_{g=1}^G$ are obtained jointly (because of the geographical component) indeterminate. This problem could be partially solved through singular value decomposition and applying a least-squares method. However, the gap between predicted and actual deaths was always significantly worse when using this alternative procedure.

it due to the consecutive-zeros problem.

For the regions that do not report daily deaths, we give daily values to ρ_g based on the reported number of daily infections. To do that, we again first omit the geographical components (i.e., $\kappa = 0$), and from equations (44) and (45) recover, for each day and region, a preliminary ρ_g from the infection data. This preliminary ρ_g serves to generate the necessary time series of predicted fatalities F_g from the system of equations (44) to (47e). Once we have the estimated deaths, we follow the method described in appendix B to get ρ_t that will be used during the simulations.

In order to start the simulations, we need initial values for different variables. Tables 6 and 7 provides some of those initial values for different economic and disease related variables, respectively. The population size N_g at the beginning of the pandemic in each region comes from the same sources as deaths (see Table 5). To be consistent with the input-output data, the rest of numbers are extracted from the year 2013. We pick the expenditure shares of intermediate goods and final products by sector, origin and destination, π_{gi}^j and Π_{gi}^j , from Thiessen (2020). The number of workers, L_g , are obtained from different sources. In particular, for the EU28, we use employment by NUTS 2 regions from regional labour statistics, Eurostat. For ROW, we take the number of persons engaged from Penn World Tables, 10.0.

Wages, w_g , are calculated as total compensation of employees divided by the employment figures. Total compensation of employees for the EU27 group (EU28 minus the United Kingdom) comes from the Eurostat regional accounts data; whereas for the UK, we get them from the gross annual pay for all employee jobs reported by Annual Survey of Hours and Earnings. For ROW, compensation of employees are directly taken from Thiessen (2020). Lump-sum taxes τ_g are calibrated so as to reproduce the observed total expenditures on final products by region and sector, X_g^j , provided by Thiessen (2020).

Subsidies for intermediate goods and final-good products/materials, s_g^j and \mathfrak{s}_g^j , respectively, are equalized to zero. Bilateral ad-valorem tariff for intermediate and final goods, τ_{gi}^j and T_{gi}^j , respectively, are zero among EU members. The only tariffs different from zero are the ones related to ROW. We assign values to the different industries using information from Eurostat (2017) on average import tariffs imposed by the EU28 to other countries in 2013 and WITS - UNCTAD TRAINS information (see appendix for details).

5 Results

We focus on the first wave of the Covid-19 pandemic, and more specifically, in the period that goes from February 25 to July 15, 2020. First, we take a look at the fatality data and the calibrated ρ_g . Figure 1 provides the total daily number of deaths in the European Union (EU27) and in the UK.

This number in our smoothed time series reached a maximum values of 2,867 in the EU27 on April 4th, and 887 in the UK on April 11th. That is, the pandemic in the UK evolved with a one-week lag compared to the European Union. Nevertheless, even the death events were larger in continental Europe, the incidence of the disease was actually larger in the UK. We can observe this fact in Figure 2 that reports the number of deaths per 100,000 inhabitants. In the UK, this ratio reached 1.25, whereas in the EU27 its maximum was a bit less than half that number, in particular it was 0.61.

Figure 3 presents the average value of the parameter ρ_g across NUTS2 regions. Remember that this parameter is calibrated as a residual, and therefore, its values capture the disease ecology but also the effect of the policies applied to fight the pandemic. We can see in Figure 3 that the probability of infection reached higher values in the UK than in the European Union. The maximum, in particular, was 0.20 on March 21st for the former economy and 0.14 on March 22nd for the latter. However, we can also see that the reduction was faster and deeper in the UK than in the EU27. That is, policies seem to have been more successful in the UK, maintaining after April 16th a gap in favor of the UK of about 2 percentage points.

Let us now have a more disaggregated view of the death data in the UK. Figure 4 plots the number of deaths in each of the 37 NUTS2 regions in the UK. The largest number of daily cases was achieved in Inner London-East (UKI2), Greater Manchester (UKD3) and West Midlands (UKG3) with 118, 64 and 57 deaths in one day, respectively. The lowest daily numbers, on the other hand, took place in North Eastern Scotland (UKM5), Highlands and Islands (UKM6) and Northern Ireland (UKNO) with 3, 3 and 4 cases, respectively.

Even though the number of deaths and their relative magnitude per 100,000 inhabitants show a high correlation of 0.561, they do not correlate perfectly. In the second column of results in Table 8, we see that the largest volumes of deaths per 100,000 inhabitants are found in Greater Manchester (UKD3), Cheshire (UKD6), Trees Valley and Durham (UKC1) and West Midlands (UKG3) with rates equal to 93, 90, 87 and 87; and the lowest in Northern Ireland (UKNO), Dorset and Somerset (UKK2) and Devon (UKK4) where these rates were 6, 19 and 22, respectively.

Our next task is analyzing what the predictions of the model say about the impact of the policy measures implemented during the first wave and captured by the evolution of the parameter ρ_g . We start by looking at how the model does at matching the fatality data. Figure 5 shows that the model predictions follow well the trend and its changes in the data. Nevertheless, they tend to underestimate the number of deaths. Comparing columns one and three in Table 8, we can see that this generates an error in the predicted total number of deaths of 19.5% and 24.8% for the European Union and the United Kingdom, respectively. This is due to the method followed to calibrate the parameter ρ_g , which does not consider the geographic component of the infection (see appendix for details).

The first question that we ask is what would have been the cost for the economy in terms of deaths if no policy had been implemented. At the regional level, the parameter ρ_g reaches its largest values at the beginning of the infection in the corresponding area, and then goes down due to the policy actions implemented. Hence, in order to answer the above question, we let the parameter ρ_g remain constant at its average over the first ten days during which region g reports fatalities. The purpose of averaging out over ten days is reducing measurement error concerns.

Table 8 in the columns labeled as “Predicted deaths with ρ constant” gives the results from this exercise. Without the policy reaction, deaths in the European Union would have been 4,545,222 instead of the predicted 107,112, and 1,248,078 instead of 30,571 in the UK. Which represent an increase rate of 4,143% and 3,983%, respectively. In terms of the lives saved per 100,000 inhabitants, the average for the EU27 and the UK equal 202 and 1718, respectively. That is, again the impact looks stronger in the UK. Across NUTS2 UK regions, there is a relatively high correlation of 0.668 between the number of deaths and the lives saved by policies. More specifically, the largest effect is found in Berkshire, Buckinghamshire and Oxfordshire (UKJ1) where 2654 lives per 100,000 inhabitants were saved by the policy measures. Other areas where more than 2000 lives per 100,000 inhabitants were saved include Cheshire (UKD6), Derbyshire and Nottinghamshire (UKF1), Greater Manchester (UKD3), Inner London-East (UKI2), West Midlands (UKG3) and Essex (UKH3). The smallest impact, in turn, is found in Lincolnshire (UKF3), North Eastern Scotland (UKM5) and Dorset and Somerset (UKK2), where the lives saved are between 849, 861 and 903 per 100,000 inhabitants, respectively.

In this paper, we are specially interested in measuring the impact of the economic links in the pandemic. Let us start by looking at the weight of trade with different locations in each of the UK regions. Table 9 says that the largest share in trade is UK based. Intra-region and cross-UK-region trade accounts for between 83.0% and 96.2% of total trade. Whether the former form of trade or the latter one dominated varies widely across regions. For example, Cheshire (UKD6) is the one that shows the largest reliance in domestic trade: 50.6% is trade within the region and 25.4% comes from flows with other UK areas. Lincolnshire (UKF3) is, on the other extreme, the one that relies the less from intra-region flows, only 28.7%, whereas its inter-regional trade with the rest of the UK accounts for 66.1% of total trade. Trade flows with the European Union also vary significantly across UK regions. The largest shares of 7.6% and 7.9% are shown by Inner London East and West (UKI1 and UKI2), whereas the lowest of 3.2% is shown by Eastern Scotland (UKM2). These results tell us that trade across regions may have had an important effect on the spread of the disease.

A first assessment of the effect of these economic links is provided in the fourth column of results in Table 8. It gives the percentage contribution of the Geographic component in equation (45) to

the generation of infected individuals, and therefore, to the number of fatalities. Recall that the Geographic component is the one that collects the impact of all economic activity. The weight of this component in total deaths is, on average, around 10%, and more specifically, 10.2% in the European Union and 9.7% in the UK. Across UK regions, it reaches the highest values of 19.6 percent in Inner London-East (UKI2), 17.0% for Eastern Scotland (UKM2) and 16.8% for Devon. The smallest one, 7.8%, corresponds to Kent (UKJ4) and North Eastern Scotland (UKM5).

The geographic component is also affected by domestic economic activity. To get a closer look at the effect of the trade relations with other nations. We consider the effect of maintaining ρ_g constant in the EU27 but not in the UK. This will give us an idea of the impact of the applied European-Union anti-Covid-19 policies on the UK prevalence. This effect in our model fully runs through economic activity. The first three columns in Table 10 provide the results of this experiment. Without the policies implemented in the EU27, the number of deaths in the UK would have been a 80% larger. The lives saved by those policies amount to 24,434 or 34 per 100,000 inhabitants.

By region, Highlands and Islands (UKM6) are the one that was benefitted the most, with lives saved per 100,000 inhabitants equal to 76. Then, Cornwall and Isles of Scilly (UKK3), Cumbria (UKD1), Northern Ireland (UKN0), North Eastern Scotland (UKM5) and Lincolnshire (UKF3) saved more than 50 lives each. The ones that benefitted the less were Greater Manchester (UKD3), West Yorkshire (UKE4), Gloucestershire, Wiltshire and Bristol/Bath area (UKK1) and West Midlands (UKG3), for which the EU27 policies saved less than 25 lives.

The last three columns in Table 10 focus exclusively on the policies implemented in the UK. They show the results when we assume that ρ_g changes only in non-UK regions. They say that UK anti-Covid-19 measures saved 50,620 lives in the European Union, which represents two lives per 100,000 inhabitants. In the UK, this number is much larger; in particular, they saved a total of 1,204,239 lives or 1,700 per 100,000 inhabitants. Berkshire, Buckinghamshire and Oxfordshire (UKJ1) was the most benefitted, with 2,649 lives saved per 100,000 inhabitants. It was followed by Cheshire (UKD6), Greater Manchester (UKD3), Derbyshire and Nottinghamshire (UKF1), Inner London-East (UKI2), West Midlands (UKG3) and Essex (UKH3); all of them with more than 2,000 lives saved by the fight against Covid-19 in the UK during the first wave. At the bottom of this ranking, we have Lincolnshire (UKF3), North Eastern Scotland (UKM5) and Dorset and Somerset (UKK2) with 808, 818 and 864 lives saved per 100,000 inhabitants, respectively. Interestingly, the correlation across UK regions between the lives saved by EU27 and by UK policies is -0.672. The reason is that the EU27 effect on the UK works exclusively through economic links, whereas the one of UK policy affects the evolution of the disease also through social interaction.

6 Conclusion

We have built a spatial model of trade with supply-chain links across NUTS2 European regions to try to understand the effect of economic links and policies in the spread of the Covid-19 pandemic during the first wave, which goes from the 25th of February to the 15th of July, 2020. Our have mainly focus on this effect within the UK.

During that period, the incidence the disease was larger in the UK than in the European Union. However, we find that the fight to reduce the infection rates was more successful in the former economy than in the latter. More importantly, without the policy reaction in Europe, the number of deaths during the first wave of the pandemic would have been about 4,400,000 larger in the European Union, and about 1,217,000 higher in the UK. In terms of the lives saved per 100,000 inhabitants, the average for the EU27 and the UK equal 202 and 1,718, respectively. On average, the largest gains where in areas where the volume of deaths was higher, like Berkshire, Buckinghamshire and Oxfordshire, Cheshire, Greater Manchester, Inner London-East, West Midlands, and Essex.

In terms of the effect of economic activity to the spread of the disease and the impact of the policy measures, we find that the percentage contribution of the Geographic component to the number of fatalities is, on average, around 10%. Hence, even though family and social interactions have a larger weight, the one of economic activity is also significant. We also find that the number of deaths in the UK in the absence of anti-Covid-19 measures in the European-Union would have been a 80% larger; they saved about 34 lives per 100,000 inhabitants. In turn, UK anti-Covid-19 measures saved 50,620 lives in the European Union, which represents two lives per 100,000 inhabitants. In the UK, this number is much larger; in particular, they saved a total of about 1,200,000 lives or 1,700 per 100,000 inhabitants.

We have just started exploiting the rich structure of the model. There is still much work that can be done to understand the effects of economic links on the spread of the disease and the capacity of the economy to recover from the recession. In future work, we plan to analyze the effect on the more recent evolution of the pandemic and on the prospects of the economy to recover of vaccination policies, telematic work, selected sectoral and regional closures, subsidies and tariffs.

References

- ACEMOGLU, D., V. CHERNOZHUKOV, I. WERNING, AND M. D. WHINSTON (2020): “Optimal Targeted Lockdowns in a Multi-Group SIR Model,” Working Paper 27102, National Bureau of Economic Research.
- ADDA, J. (2016): “Economic Activity and the Spread of Viral Diseases: Evidence from High Frequency Data *,” *The Quarterly Journal of Economics*, 131(2), 891–941.
- ALLEN, T., AND C. ARKOLAKIS (2014): “Trade and the Topography of the Spatial Economy,” *The Quarterly Journal of Economics*, 129(3), 1085–1140.
- ALVAREZ, F. E., D. ARGENTE, AND F. LIPPI (2020): “A Simple Planning Problem for COVID-19 Lockdown,” Working Paper 26981, National Bureau of Economic Research.
- ANTRÀS, P., S. J. REDDING, AND E. ROSSI-HANSBERG (2020): “Globalization and Pandemics,” Working Paper 27840, National Bureau of Economic Research.
- CALIENDO, L., AND F. PARRO (2014): “Estimates of the Trade and Welfare Effects of NAFTA,” *The Review of Economic Studies*, 82(1), 1–44.
- CALIENDO, L., F. PARRO, E. ROSSI-HANSBERG, AND P.-D. SARTE (2017): “The Impact of Regional and Sectoral Productivity Changes on the U.S. Economy,” *The Review of Economic Studies*, 85(4), 2042–2096.
- ÇAKMAKLI, C., S. DEMIRALP, C. KALEMLİ-ÖZCAN, S. YEŞİLTAŞ, AND M. A. YILDIRIM (2021): “The Economic Case for Global Vaccinations: An Epidemiological Model with International Production Networks,” Working Paper 28395, National Bureau of Economic Research.
- CHAKRABORTY, S., C. PAPAGEORGIOU, AND F. PÉREZ-SEBASTIÁN (2010): “Diseases, infection dynamics, and development,” *Journal of Monetary Economics*, 57(7), 859 – 872.
- DE VET, J. M., D. NIGOHOSYAN, J. N. FERRER, A.-K. GROSS, S. KUEHL, AND M. FLICKENSCHILD (2021): “Impacts of the COVID-19 pandemic on EU industries,” Publication for the committee on industry, research and energy, policy department for economic, scientific and quality of life policies, European Parliament, Luxembourg.
- DESMET, K., AND R. WACZIARG (2021): “JUE Insight: Understanding spatial variation in COVID-19 across the United States,” *Journal of Urban Economics*, p. 103332.
- DINGEL, J. I., AND B. NEIMAN (2020): “How Many Jobs Can be Done at Home?,” Working Paper 26948, National Bureau of Economic Research.

- EATON, J., AND S. KORTUM (2002): “Technology, Geography, and Trade,” *Econometrica*, 70(5), 1741–1779.
- EICHENBAUM, M. S., S. REBELO, AND M. TRABANDT (2020): “The Macroeconomics of Epidemics,” Working Paper 26882, National Bureau of Economic Research.
- EUROSTAT (2017): *Globalisation patterns in EU trade and investment*. Publications Office of the European Union, Luxembourg.
- FAJGELBAUM, P., A. KHANDELWAL, W. KIM, C. MANTOVANI, AND E. SCHAAL (2020): “Optimal Lockdown in a Commuting Network,” Working Paper 27441, National Bureau of Economic Research.
- FERNANDEZ-VILLAYERDE, J., AND C. I. JONES (2020): “Estimating and Simulating a SIRD Model of COVID-19 for Many Countries, States, and Cities,” Working Paper 27128, National Bureau of Economic Research.
- FOGLI, A., AND L. VELDKAMP (2021): “Germs, Social Networks, and Growth,” *The Review of Economic Studies*, rdab008.
- GLOVER, A., J. HEATHCOTE, D. KRUEGER, AND J.-V. RIOS-RULL (2020): “Health versus Wealth: On the Distributional Effects of Controlling a Pandemic,” Working Paper 27046, National Bureau of Economic Research.
- GUERRIERI, V., G. LORENZONI, L. STRAUB, AND I. WERNING (2020): “Macroeconomic Implications of COVID-19: Can Negative Supply Shocks Cause Demand Shortages?,” Working Paper 26918, National Bureau of Economic Research.
- HEFFERNAN, J., R. SMITH, AND L. WAHL (2005): “Perspectives on the basic reproductive ratio,” *Journal of The Royal Society Interface*, 2(4), 281–293.
- HERRENDORF, B., R. ROGERSON, AND Á. VALENTINYI (2013): “Two Perspectives on Preferences and Structural Transformation,” *American Economic Review*, 103(7), 2752–89.
- JORDA, O., S. R. SINGH, AND A. M. TAYLOR (2020): “Longer-Run Economic Consequences of Pandemics,” Working Paper 2020-09, Federal Reserve Bank of San Francisco.
- KEELING, M. J. (1999): “The effects of local spatial structure on epidemiological invasions,” *Proceedings of the Royal Society of London. Series B: Biological Sciences*, 266(1421), 859–867.
- KERMACK, W. O., A. G. MCKENDRICK, AND G. T. WALKER (1927): “A contribution to the mathematical theory of epidemics,” *Proceedings of the Royal Society of London. Series A, Containing Papers of a Mathematical and Physical Character*, 115(772), 700–721.

- KRUEGER, D., H. UHLIG, AND T. XIE (2020): “Macroeconomic Dynamics and Reallocation in an Epidemic: Evaluating the “Swedish Solution,” Working Paper 27047, National Bureau of Economic Research.
- LLOYD, A. L., AND R. M. MAY (1996): “Spatial Heterogeneity in Epidemic Models,” *Journal of Theoretical Biology*, 179(1), 1–11.
- MAYER, J. D. (2000): “Geography, ecology and emerging infectious diseases,” *Social Science & Medicine*, 50(7), 937–952.
- OSTER, E. (2012): “Routes of Infection: Exports and HIV Incidence in Sub-Saharan Africa,” *Journal of the European Economic Association*, 10(5), 1025–1058.
- PAENG, S.-H., AND J. LEE (2017): “Continuous and discrete SIR-models with spatial distributions,” *Journal of mathematical biology*, 74(7), 1709–1727.
- PERSYN, D., J. DIAZ-LANCHAS, J. BARBERO, A. CONTE, AND S. SALOTTI (2019): “A new dataset of distance and time related transport costs for EU regions,” Working Paper JRC119412, Territorial Development Insights Series, European Commission.
- SHEEHAN, M. M., A. J. REDDY, AND M. B. ROTHBERG (2021): “Reinfection Rates Among Patients Who Previously Tested Positive for Coronavirus Disease 2019: A Retrospective Cohort Study,” *Clinical Infectious Diseases*, ciab234.
- THIESSEN, M. (2020): “RHOMOLO-IO dset 2013,” Discussion paper, European Commission, Joint Research Centre (JRC), [Dataset] PID: <http://data.europa.eu/89h/9559442f-a88e-484b-934d-fa4bbd5e6663>.
- VILLANI, L., M. MCKEE, F. CASCINI, W. RICCIARDI, AND S. BOCCIA (2020): “Comparison of deaths rates for COVID-19 across Europe during the first wave of the COVID-19 pandemic,” *Frontiers in Public Health*, 8.
- WILSON, M. E. (2010): “Chapter 101 - Geography of infectious diseases,” in *Infectious Diseases (Third Edition)*, ed. by J. Cohen, S. M. Opal, and W. G. Powderly, pp. 1055–1064. Mosby, London, third edition edn.
- WORLD BANK (2009): *World development report 2009: Reshaping economic geography*. The World Bank.

A The Basic Reproduction Number in Our SVIRCF Model

Following [Heffernan, Smith, and Wahl \(2005\)](#), we can write the equation for infected individuals in matrix form as:

$$\mathbf{I}' = (\mathbb{I} + \mathbf{F} - \mathbf{D}) \mathbf{I}; \quad (50)$$

where \mathbb{I} is the identity matrix, \mathbf{I}' is the vector of infections in each location at time $t + 1$, and \mathbf{F} and \mathbf{D} are defined as

$$\mathbf{F} = \begin{pmatrix} (1-\kappa)\rho_1 \frac{S_1}{N_1} + \kappa\Lambda_1\rho_1 \tilde{X}_{11} \frac{S_1}{N_1} & \cdots & \kappa\Lambda_g\rho_g \tilde{X}_{g1} \frac{S_1}{N_g} & \cdots & \kappa\Lambda_G\rho_G \tilde{X}_{G1} \frac{S_1}{N_G} \\ \vdots & \ddots & \vdots & \ddots & \vdots \\ \kappa\Lambda_1\rho_1 \tilde{X}_{1g} \frac{S_g}{N_1} & \cdots & (1-\kappa)\rho_g \frac{S_g}{N_g} + \kappa\Lambda_g\rho_g \tilde{X}_{gg} \frac{S_g}{N_g} & \cdots & \kappa\Lambda_G\rho_G \tilde{X}_{Gg} \frac{S_g}{N_G} \\ \vdots & \ddots & \vdots & \ddots & \vdots \\ \kappa\Lambda_1\rho_1 \tilde{X}_{1G} \frac{S_G}{N_1} & \cdots & \kappa\Lambda_g\rho_g \tilde{X}_{gG} \frac{S_G}{N_g} & \cdots & (1-\kappa)\rho_G \frac{S_G}{N_G} + \kappa\Lambda_G\rho_G \tilde{X}_{GG} \frac{S_G}{N_G} \end{pmatrix}$$

$$\mathbf{D} = \begin{pmatrix} \varphi & \cdots & 0 & \cdots & 0 \\ \vdots & \ddots & \cdots & \ddots & \vdots \\ 0 & \cdots & \varphi & \cdots & 0 \\ \vdots & \ddots & \cdots & \ddots & \vdots \\ 0 & \cdots & 0 & \cdots & \varphi \end{pmatrix}$$

For the two region case, these matrices equal:

$$\mathbf{F} = \begin{pmatrix} (1-\kappa)\rho_1 \frac{S_1}{N_1} + \kappa\Lambda_1\rho_1 \tilde{X}_{11} \frac{S_1}{N_1} & \kappa\Lambda_2\rho_2 \tilde{X}_{21} \frac{S_1}{N_2} \\ \kappa\Lambda_1\rho_1 \tilde{X}_{12} \frac{S_2}{N_1} & (1-\kappa)\rho_2 \frac{S_2}{N_2} + \kappa\Lambda_2\rho_2 \tilde{X}_{22} \frac{S_2}{N_2} \end{pmatrix}$$

$$\mathbf{V} = \begin{pmatrix} \varphi & 0 \\ 0 & \varphi \end{pmatrix}$$

Let us keep focusing on the simplest case of two regions for which the components of \tilde{X}_{gi} do not change over time, neither the parameters regarding the disease ecology. In addition, assume that $S_{m,t} = N_{m,t}$ and there is no vaccine available. Then, we have that the basic reproduction number \mathcal{R}_0 is given by the largest eigenvalue of matrix $\mathbf{B} = \mathbf{FV}^{-1}$. Matrix \mathbf{B} is given by

$$\mathbf{B} = \begin{pmatrix} \frac{\tilde{X}_{11}\kappa\rho\Lambda + \rho(1-\kappa)}{\varphi} & \frac{\tilde{X}_{21}\kappa\rho\Lambda}{\varphi} \\ \frac{\tilde{X}_{12}\kappa\rho\Lambda}{\varphi} & \frac{\tilde{X}_{22}\kappa\rho\Lambda + \rho(1-\kappa)}{\varphi} \end{pmatrix}$$

and the basic reproduction number is given by

$$\mathcal{R}_0 = \frac{\kappa\rho\Lambda\sqrt{\tilde{X}_{11}^2 - 2\tilde{X}_{11}\tilde{X}_{22} + 4\tilde{X}_{12}\tilde{X}_{21} + \tilde{X}_{22}^2}}{2\varphi} + \frac{\rho(\tilde{X}_{11}\kappa\Lambda + \tilde{X}_{22}\kappa\Lambda - 2\kappa + 2)}{2\varphi}$$

(There seem to be subindices missing in $\rho\Lambda$) which increases with trade integration, since the partial derivatives are increasing in the trade share with the opposite region.

$$\frac{\partial \mathcal{R}_0}{\partial \tilde{X}_{12}} = \frac{\kappa\rho\Lambda\tilde{X}_{21}}{\varphi\sqrt{\tilde{X}_{11}^2 - 2\tilde{X}_{11}\tilde{X}_{22} + 4\tilde{X}_{12}\tilde{X}_{21} + \tilde{X}_{22}^2}} > 0$$

$$\frac{\partial \mathcal{R}_0}{\partial \tilde{X}_{21}} = \frac{\kappa\rho\Lambda\tilde{X}_{12}}{\varphi\sqrt{\tilde{X}_{11}^2 - 2\tilde{X}_{11}\tilde{X}_{22} + 4\tilde{X}_{12}\tilde{X}_{21} + \tilde{X}_{22}^2}} > 0$$

B Parameters for the Evolution of the Disease

In order to calibrate $\{\rho_{gt}\}_{g=1}^G$, we follow the method in [Fernandez-Villaverde and Jones \(2020\)](#) and recover the parameter from deaths numbers. In addition, to ameliorate possible mismeasurement problems, like for example underreporting during weekends, we first smooth those daily-deaths series using a moving average of seven days and then a Hodrick-Prescott filter with smoothing parameter 850.

This calibration method is applied to our case as follows. Let us add a time index (t) to the different variables for mathematical convenience. Additionally, let us take the convention that Z_t provides the value of an arbitrary variable Z at the end of period t , and that $\Delta Z_{t+1} = Z_{t+1} - Z_t$.¹⁰ Define also $f_{gt+1} \equiv \Delta F_{gt+1}$, that is, the (smoothed) number of people that died on day $t+1$ in region g . For the initial waves of the pandemic, in which there was no vaccine available, we assume $\lambda_g = 0$ for all regions.

From equation (47e), we can solve for R_{gt} in terms of daily deaths as

$$R_{gt} = \frac{f_{gt+1}}{\delta \xi}, \quad (51)$$

which then implies

$$\Delta R_{gt+1} = \frac{\Delta f_{gt+2}}{\delta \xi}. \quad (52)$$

Combining equations (47c) and (52), we can express infected individuals today as a function of future daily fatalities:

$$I_{gt} = \frac{1}{\delta \varphi} \left(\frac{\Delta f_{gt+2}}{\xi} + f_{gt+1} \right). \quad (53)$$

Which implies

$$\Delta I_{gt+1} = \frac{1}{\delta \varphi} \left(\frac{\Delta f_{gt+3} - \Delta f_{gt+2}}{\xi} + \Delta f_{gt+2} \right). \quad (54)$$

Using the ratio of (54) to (53), the growth rate of the infected cases can be obtained as:

$$\frac{\Delta I_{gt+1}}{I_{gt}} = \frac{1/\xi(\Delta f_{gt+3} - \Delta f_{gt+2}) + \Delta f_{gt+2}}{1/\xi \Delta f_{gt+2} + f_{gt+1}}. \quad (55)$$

Next, equation (44), letting $G_{gt}(I_{it})$ denote the geographic component in equation (45), delivers

$$(1 - \kappa)\rho_{gt} + \frac{\kappa G_{gt}(I_{it})N_{gt}}{I_{gt}} = \frac{N_{gt}}{S_{gt}} \left(\frac{\Delta I_{gt+1}}{I_{gt}} + \varphi \right).$$

Which substituting (53) and (55) becomes:

$$(1 - \kappa)\rho_{gt} + \kappa G_{gt}(I_{it}) \frac{\delta \varphi N_{gt}}{\left(\frac{\Delta f_{gt+2}}{\xi} + f_{gt+1} \right)} = \frac{N_{gt}}{S_{gt}} \left(\frac{1/\xi(\Delta f_{gt+3} - \Delta f_{gt+2}) + \Delta f_{gt+2}}{1/\xi \Delta f_{gt+2} + f_{gt+1}} + \varphi \right). \quad (56)$$

¹⁰Notice that the timing convention does not have any important implication for our previous discussion. It would simply mean, for example, that when the susceptible is infected by the virus or vaccinated during period t , it does not develop the disease or gets immunity until period $t+1$; and that, since L_{gt} is then the number of workers available at the end of period t , all the economic activity takes place at the end of each period.

To get an expression for the evolution of the susceptible as a function of the fatalities, we can use (47a), (45) and (53) to obtain the law of motion for this variable as:

$$S_{gt+1} = S_{gt} \left\{ 1 - \lambda_{gt} - (1 - \kappa) \frac{\rho_{gt}}{\delta \varphi N_{gt}} \left(\frac{\Delta f_{gt+2}}{\xi} + f_{gt+1} \right) + \right. \\ \left. \kappa \left(\sum_{i \in G} \tilde{X}_{ig} l_{it} \rho_{it} \frac{1}{\delta \varphi N_{it}} \left(\frac{\Delta f_{it+2}}{\xi} + f_{it+1} \right) \right) \right\} + \alpha^C C_{gt} + \alpha^V V_{gt}.$$

Note we also need to include the law of motion for vaccinated and recovered individuals which from (47b) and substituting equation (51) into (47d) yield

$$V_{gt+1} = (1 - \alpha^V) V_{gt} + \lambda_{gt} S_{gt} \quad (57)$$

$$C_{gt+1} = (1 - \alpha^C) C_{gt} + \frac{1 - \delta}{\delta} f_{gt+1} \quad (58)$$

Finally, we need initial values for $\{I_{g0}, S_{g0}, N_{g0}\}_{g=1}^G$. For the stock of fatalities, recovered and vaccinated, this value is zero, that is, $F_{g0} = C_{g0} = V_{g0} = 0$. Knowing the number of fatalities in the next two periods, we then obtain I_{g0} and R_{g0} from (53) and (51); and the number of susceptible is directly obtained from (1) taking $N_{gt} = N_{g0}$ for all t from the sources reported in Table 5.

In principle, knowing those numbers, and taking the daily deaths and fraction of vaccinated $\{f_{gt}, \lambda_{gt}\}_{g=1, t=1}^{G, \mathfrak{T}}$ from the data, we could end up with a system of four *times* G equations, given by (56) to (58), and four *times* G unknowns, $\{\rho_{gt}, S_{gt+1}, C_{gt+1}, V_{gt+1}\}_{g=1}^G$ that is solvable. However, the large number of zero deaths encountered in many periods make the system indeterminate many times when the geographical component is considered. The solution that we have adopted to solve this problem is assuming in the calibration of ρ_g that $\kappa = 0$. In this way, the system for each region simplifies and becomes independent of other areas. Hence, for each period $t \in [1, \mathfrak{T}]$ and region $g \in [1, G]$, we first recover ρ_{gt} from (56) and then $\{S_{gt+1}, C_{gt+1}, V_{gt+1}\}_{g=1}^G$ from the other three equations.

Figure 1: Total daily deaths in the EU27 and the UK

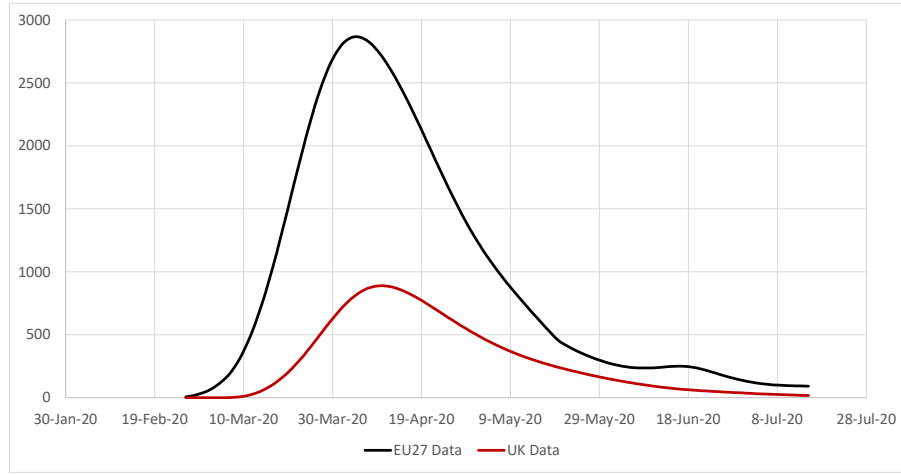


Figure 2: Daily deaths per 100,000 inhabitants in the EU27 and the UK

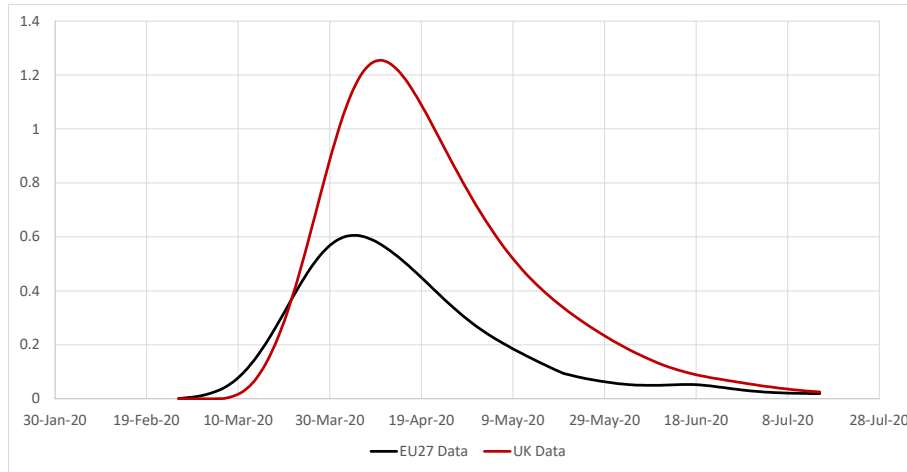


Figure 3: Average daily ρ_g in the EU27 and the UK

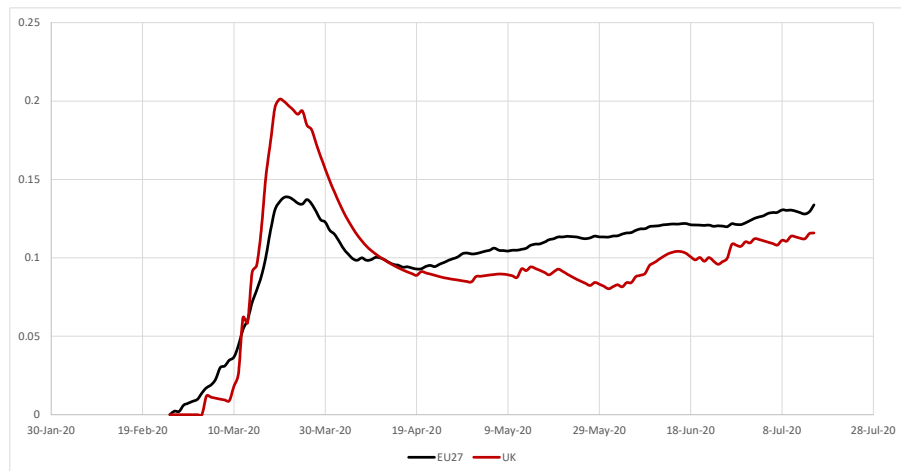


Figure 4: Total daily deaths in the UK NUTS2 regiones

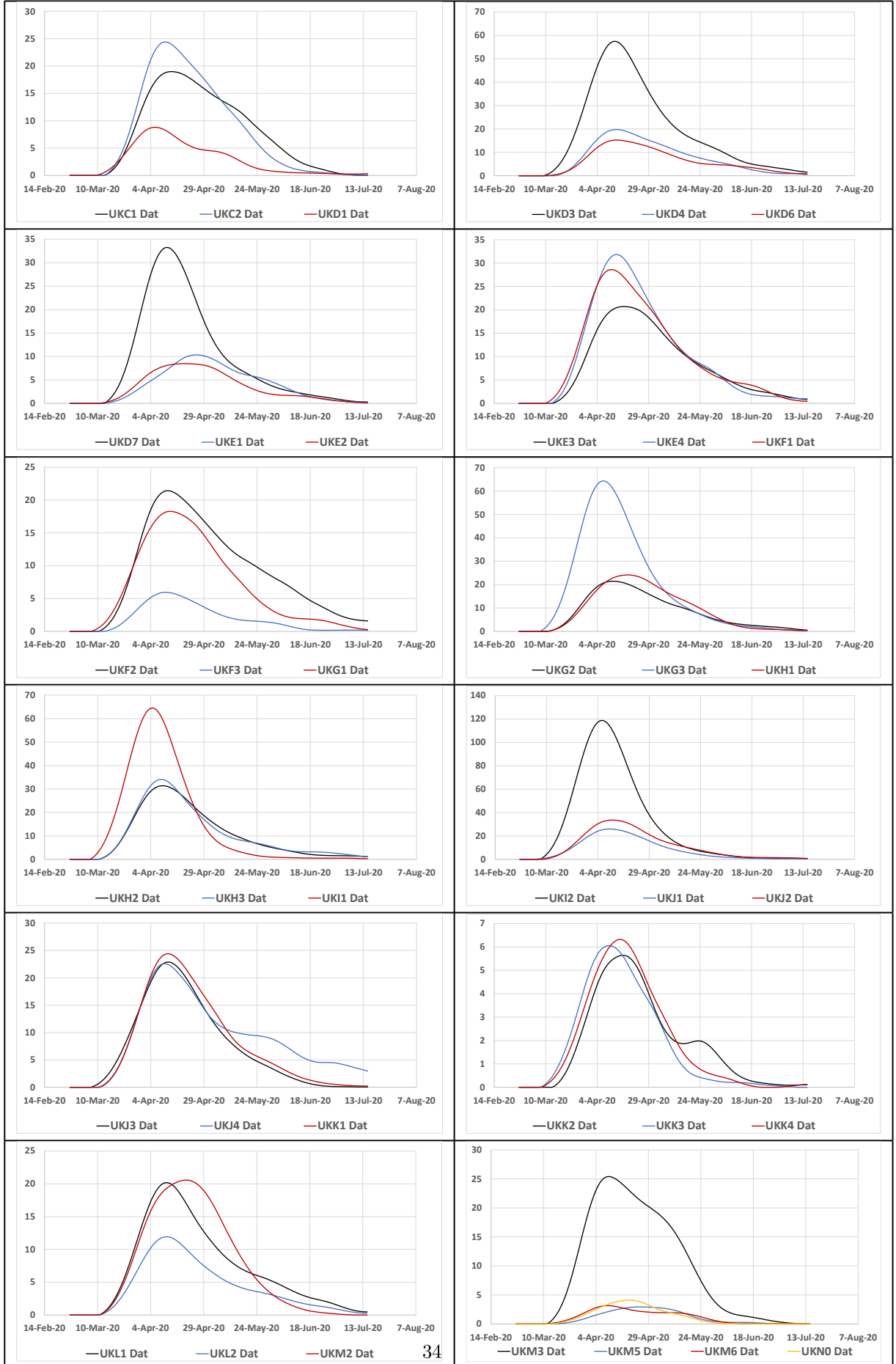


Figure 5: Daily deaths: data versus predictions

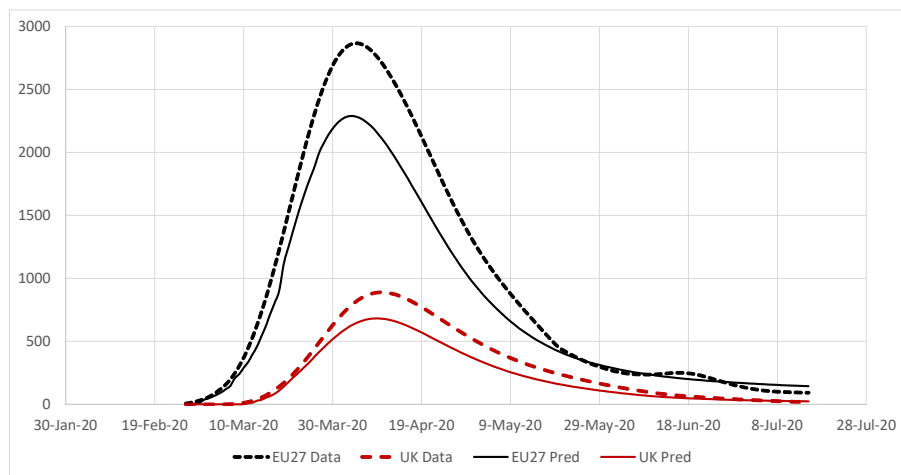


Table 1: NUTS2-2010 regions included in the analysis

Region codes	Region names	Region codes	Region names
AT11	Burgenland (AT)	DEF0	Schleswig-Holstein
AT12	Niederösterreich	DEG0	Thüringen
AT13	Wien	DK01	Hovedstaden
AT21	Kärnten	DK02	Sjælland
AT22	Steiermark	DK03	Syddanmark
AT31	Oberösterreich	DK04	Midtjylland
AT32	Salzburg	DK05	Nordjylland
AT33	Tirol	EE00	Eesti
AT34	Vorarlberg	EL11	Anatoliki Makedonia, Thraki
BE1	Région Bruxelles-Capitale / Brussels H G	EL12	Kentriki Makedonia
BE2 *	Vlaams Gewest	EL13	Dytiki Makedonia
BE3 *	Région wallonne	EL14	Thessalia
BG *	Bulgaria	EL21	Ipeiros
CYP	Kypros	EL22	Ionia Nisia
CZ01	Praha	EL23	Dytiki Ellada
CZ02	Střední Čechy	EL24	Stereia Ellada
CZ03	Jihozápad	EL25	Peloponnisos
CZ04	Severozápad	EL30	Attiki
CZ05	Severovýchod	EL41	Voreio Aigaio
CZ06	Jihovýchod	EL42	Notio Aigaio
CZ07	Střední Morava	EL43	Kriti
CZ08	Moravskoslezsko	ES11	Galicie
DE11	Stuttgart	ES12	Principado de Asturias
DE12	Karlsruhe	ES13	Cantabria
DE13	Freiburg	ES21	País Vasco
DE14	Tübingen	ES22	Comunidad Foral de Navarra
DE21	Oberbayern	ES23	La Rioja
DE22	Niederbayern	ES24	Aragón
DE23	Oberpfalz	ES30	Comunidad de Madrid
DE24	Oberfranken	ES41	Castilla y León
DE25	Mittelfranken	ES42	Castilla-la Mancha
DE26	Unterfranken	ES43	Extremadura
DE27	Schwaben	ES51	Cataluña
DE30	Berlin	ES52	Comunidad Valenciana
DE40	Brandenburg	ES53	Illes Balears
DE50	Bremen	ES61	Andalucía
DE60	Hamburg	ES62	Región de Murcia
DE71	Darmstadt	ES63	Ciudad Autónoma de Ceuta (ES)
DE72	Gießen	ES64	Ciudad Autónoma de Melilla (ES)
DE73	Kassel	ES70	Canarias (ES)
DE80	Mecklenburg-Vorpommern	FI19	Länsi-Suomi
DE91	Braunschweig	FI1B	Helsinki-Uusimaa
DE92	Hannover	FI1C	Etelä-Suomi
DE93	Lüneburg	FI1D	Pohjois- ja Itä-Suomi
DE94	Weser-Ems	FI20	Åland
DEA1	Düsseldorf	FR10	Île de France
DEA2	Köln	FR21	Champagne-Ardenne
DEA3	Münster	FR22	Picardie
DEA4	Detmold	FR23	Haute-Normandie
DEA5	Arnsberg	FR24	Centre (FR)
DEB1	Koblenz	FR25	Basse-Normandie
DEB2	Trier	FR26	Bourgogne
DEB3	Rheinessen-Pfalz	FR30	Nord - Pas-de-Calais
DEC0	Saarland	FR41	Lorraine
DED2	Dresden	FR42	Alsace
DED4	Chemnitz	FR43	Franche-Comté
DED5	Leipzig	FR51	Pays de la Loire
DEE0	Sachsen-Anhalt	FR52	Bretagne

* The NUTS2 regions were aggregated to upper levels due to lack of data

Table 1: NUTS2-2010 regions included in the analysis (continued)

Region codes	Region names	Region codes	Region names
FR53	Poitou-Charentes	PT18	Alentejo
FR61	Aquitaine	PT20	Região Autónoma dos Açores (PT)
FR62	Midi-Pyrénées	PT30	Região Autónoma da Madeira (PT)
FR63	Limousin	RO *	Romania
FR71	Rhône-Alpes	ROW	Rest of the world
FR72	Auvergne	SE11	Stockholm
FR81	Languedoc-Roussillon	SE12	Östra Mellansverige
FR82	Provence-Alpes-Côte d'Azur	SE21	Småland med öarna
FR83	Corse	SE22	Sydsverige
HRV *	Croatia	SE23	Västsverige
HU *	Hungary	SE31	Norra Mellansverige
IE *	Ireland	SE32	Mellersta Norrland
ITC1	Piemonte	SE33	Övre Norrland
ITC2	Valle d'Aosta/Vallée d'Aoste	SI01	Vzhodna Slovenija
ITC3	Liguria	SI02	Zahodna Slovenija
ITC4	Lombardia	SK01	Bratislavský kraj
ITF1	Abruzzo	SK02	Západné Slovensko
ITF2	Molise	SK03	Stredné Slovensko
ITF3	Campania	SK04	Východné Slovensko
ITF4	Puglia	UKC1	Tees Valley and Durham
ITF5	Basilicata	UKC2	Northumberland and Tyne and Wear
ITF6	Calabria	UKD1	Cumbria
ITG1	Sicilia	UKD3	Greater Manchester
ITG2	Sardegna	UKD4	Lancashire
ITH1	Provincia Autonoma di Bolzano/Bozen	UKD6	Cheshire
ITH2	Provincia Autonoma di Trento	UKD7	Merseyside
ITH3	Veneto	UKE1	East Yorkshire and Northern Lincolnshire
ITH4	Friuli-Venezia Giulia	UKE2	North Yorkshire
ITH5	Emilia-Romagna	UKE3	South Yorkshire
ITI1	Toscana	UKE4	West Yorkshire
ITI2	Umbria	UKF1	Derbyshire and Nottinghamshire
ITI3	Marche	UKF2	Leicestershire, Rutland and Northamptonshire
ITI4	Lazio	UKF3	Lincolnshire
LTU	Lietuva	UKG1	Herefordshire, Worcestershire and Warwickshire
LUX	Luxembourg	UKG2	Shropshire and Staffordshire
LVA	Latvija	UKG3	West Midlands
MLT	Malta	UKH1	East Anglia
NL *	Netherlands	UKH2	Bedfordshire and Hertfordshire
PL11	Lódzkie	UKH3	Essex
PL12	Mazowieckie	UKI1	Inner London - West
PL21	Malopolskie	UKI2	Inner London - East
PL22	Slaskie	UKJ1	Berkshire, Buckinghamshire and Oxfordshire
PL31	Lubelskie	UKJ2	Surrey, East and West Sussex
PL32	Podkarpackie	UKJ3	Hampshire and Isle of Wight
PL33	Swietokrzyskie	UKJ4	Kent
PL34	Podlaskie	UKK1	Gloucestershire, Wiltshire and Bristol/Bath area
PL41	Wielkopolskie	UKK2	Dorset and Somerset
PL42	Zachodniopomorskie	UKK3	Cornwall and Isles of Scilly
PL43	Lubuskie	UKK4	Devon
PL51	Dolnoslaskie	UKL1	West Wales and The Valleys
PL52	Opolskie	UKL2	East Wales
PL61	Kujawsko-Pomorskie	UKM2	Eastern Scotland
PL62	Warminsko-Mazurskie	UKM3	South Western Scotland
PL63	Pomorskie	UKM5	North Eastern Scotland
PT11	Norte	UKM6	Highlands and Islands
PT15	Algarve	UKN0	Northern Ireland (UK)
PT16	Centro (PT)		
PT17	Área Metropolitana de Lisboa		

* The NUTS2 regions were aggregated to upper levels due to lack of data

Table 2: NACE Rev2 sectors included in the analysis

Sections	Industries
A	Agriculture, forestry and fishing
B_E	Industry (except construction and mining)
C	Mining
F	Construction
G_I	Wholesale and retail trade, transport, accommodation and food service activities
J	Information and communication
K_L	Financial, insurance, and real estate activities
M_N	Professional, scientific, technical, administrative and support service activities
O_Q	Public administration, defence, education, human health and social work activities
R_U	Arts, entertainment and recreation; other service activities; activities of household and extra-territorial organizations and bodies

Table 3: calibration summary

Parameter	Source	Value Description
α_g^j	Thiessen (2020)	Share of sector j in total consumption expenditure in location g
γ_g^j	Thiessen (2020)	Share of value added in gross output
γ_{kj}^g	Thiessen (2020)	Input-output coefficients
θ^i, Θ^j	Thiessen (2020) and Persyn et al. (2019)	Gravity equation estimation
A_g	Dingel and Neiman (2020)	Estimated using data on who can work from home and trade shares
κ	Eichenbaum et al (202)	0.17 Average infection rate related to work
φ	Fernandez-Villaverde and Jones (2020)	0.125 Average infections per period. Then $1/\phi = 8$ days
ξ	Fernandez-Villaverde and Jones (2020)	0.143 Average number of days to resolve. Then, $1/\xi = 7$ days
δ	Fernandez-Villaverde and Jones (2020)	0.01 Average fatality rate
λ_g	Direct data on vaccinations	Estimated by regions
α^v	Several sources	0.159 Evidence on vaccine effectiveness
α^c	Several sources	0.168 Evidence on reinfection rates
ρ_g	Fernandez-Villaverde and Jones (2020)	Time varying infection rate calibrated as a residual using the model

Table 4: sector-specific shape parameters of the Fréchet distributions

Sectors	Theta_Intermediates	Theta_Finals
A	2.7776	2.7754
B_E	2.8126	2.8036
C	1.9930	1.9428
F	3.0822	3.0822
G_I	2.7182	2.7420
J	2.7242	2.6601
K_L	2.9438	2.9439
M_N	2.8146	2.8298
O_Q	3.0900	3.0903
R_U	3.0257	3.0228

Table 5: death and infection data sources per country

Country	Country code	Number of regions	Indicator*	Source
Austria	AT	9	Deaths	AGES
Belgium	BE	3	Deaths	Sciensano
Bulgaria	BG	1	Deaths	Our World In Data
Croatia	HR	1	Deaths	Our World In Data
Cyprus	CY	1	Deaths	Our World In Data
Czech Republic	CZ	8	Deaths	Ministry of Health
Denmark	DK	5	Infections	Statens Serum Institut
Estonia	EE	1	Deaths	Our World In Data
Finland	FI	5	Deaths	Helsing Sanomat
France	FR	22	Deaths	Government Statistical Office
Germany	DE	38	Deaths	Robert Koch Institute
Greece	EL	13	Infections	Ministry of Health
Hungary	HU	1	Deaths	Our World In Data
Ireland	IE	1	Deaths	Our World In Data
Italy	IT	21	Deaths	Dipartimento della Protezione Civile
Latvia	LV	1	Deaths	Our World In Data
Lithuania	LT	1	Deaths	Our World In Data
Luxembourg	LU	1	Deaths	Our World In Data
Malta	MT	1	Deaths	Our World In Data
Netherlands	NL	1	Deaths	Our World In Data
Poland	PL	16	Deaths	Government of Poland
Portugal	PT	7	Deaths	Ministry of Health
Rest of the World	ROW	1	Infections	Our World In Data
Romania	RO	2	Deaths	Our World In Data
Slovakia	SK	4	Infections	Radovan Ondas**
Slovenia	SI	2	Deaths	COVID-19 Sledilnik
Spain	ES	19	Deaths	Narrativa Tracking
Sweden	SE	8	Deaths	Public Health Agency of Sweden
United Kingdom	UK	37	Infections	National Health Service

* Population numbers at the time when the pandemic started come from the same sources.

** Radovan Ondas independently compiled a machine readable dataset from the reports published by the National Health Information Centre. The data is accessible in his GitHub Repository: <https://github.com/radoondas/covid-19-slovakia/>

Table 6: values for certain economic variables in the initial period

Regions	Employment (,000)	Wages (,000)	Tax per capita	Regions	Employment (,000)	Wages (,000)	Tax per capita
AT11	134	26.5821	-7.2633	DEF0	1336.9	29.4306	-1.0281
AT12	782.3	30.3157	-12.2176	DEG0	1067.1	26.5895	0.7949
AT13	796.1	51.7636	-15.2691	DK01	858.4	61.7700	-17.9257
AT21	257.5	33.9612	-11.4699	DK02	367.7	37.3745	-10.0792
AT22	584.6	34.5074	-10.7816	DK03	538.9	47.2973	-21.9573
AT31	719.2	37.1969	-17.7329	DK04	606	46.6467	-19.7161
AT32	273.8	39.2586	-22.7968	DK05	265.2	45.5326	-22.0819
AT33	369.8	34.6403	-20.1357	EE00	621.3	13.8727	-8.7107
AT34	187.4	36.0726	-23.4575	EL11	187.4	13.9749	-1.2872
BE10	412.6	96.7746	-15.8892	EL12	553.6	15.5690	-2.5216
BE20	2774.6	41.1520	-15.0507	EL13	77.1	22.5546	-10.0949
BE30	1343.2	36.6868	-2.7465	EL14	235.5	13.8855	-2.7245
BG00	2934.9	5.6618	-3.4726	EL21	103.9	13.5129	-1.5752
CYP	365.1	22.8508	-10.6850	EL22	75.2	13.7773	-6.0525
CZ01	649.4	27.0746	-22.3040	EL23	202.7	13.8518	-3.9175
CZ02	626.2	10.4313	-4.1040	EL24	171.3	15.6482	-7.4496
CZ03	576.1	11.7867	-4.4123	EL25	191.3	13.4721	-3.3042
CZ04	504.8	10.1360	-3.7595	EL30	1312	22.3998	-11.0830
CZ05	689.5	11.2797	-2.7009	EL41	65.6	14.6520	-1.1546
CZ06	792.9	12.6581	-5.7872	EL42	122.8	17.2248	-7.8097
CZ07	554.2	11.2322	-2.1210	EL43	214.8	14.1792	-5.4247
CZ08	544.1	12.3791	-4.6760	ES11	1006.4	23.0889	-9.8079
DE11	2024.8	46.4185	-19.4286	ES12	369.4	25.6050	-8.7703
DE12	1382.3	40.4823	-7.5977	ES13	222.5	23.6975	-7.9710
DE13	1141.4	33.8518	0.6914	ES21	873.6	33.2188	-10.6814
DE14	943.3	37.0806	1.3750	ES22	258.1	30.6304	-11.0285
DE21	2376.5	44.9057	-30.3063	ES23	124.5	24.6482	-13.3054
DE22	626	31.7061	3.1370	ES24	515.3	27.5587	-11.0604
DE23	566.2	34.7086	4.3142	ES30	2718.1	35.5904	-12.6868
DE24	542.5	33.6627	6.0943	ES41	916.4	24.1794	-7.9359
DE25	864.6	41.9546	3.7367	ES42	712.3	21.3244	-8.2121
DE26	674.6	34.3751	3.4374	ES43	339.7	21.7748	-4.2174
DE27	919.4	34.9232	0.7611	ES51	2969.6	29.9354	-11.5671
DE30	1604.1	36.5346	-9.2814	ES52	1771.2	23.2228	-8.0898
DE40	1200.1	24.8842	-19.8731	ES53	475.8	23.4256	-10.6539
DE50	299.1	51.2956	2.6229	ES61	2571.5	23.6645	-6.0529
DE60	885.6	54.9938	-18.5391	ES62	514.9	23.3022	-12.7789
DE71	1912.2	45.9633	-37.1080	ES63	25.6	33.8906	-0.3815
DE72	503.5	33.9545	5.7147	ES64	24.6	31.5407	0.0139
DE73	591.4	37.5593	4.6166	ES70	729.7	24.0643	-7.0549
DE80	741.9	26.4571	1.9778	FI19	600.6	38.1363	-73.2872
DE91	734	40.7403	2.9661	FI1B	796.1	48.4994	1.8983
DE92	1013.5	35.9496	-0.4578	FI1C	502.2	37.1915	3.0587
DE93	804.8	24.6945	2.3407	FI1D	542.9	36.3672	1.1617
DE94	1214.6	30.5228	-5.3343	FI20	15	47.6613	6.3367
DEA1	2364	40.9027	-31.2466	FR10	5277.6	64.7503	-17.3524
DEA2	2013.5	40.1806	-29.2722	FR21	506.9	37.2000	-5.5220
DEA3	1209.3	32.5144	-4.4063	FR22	728	34.1721	-1.1953
DEA4	968.6	35.6644	0.6930	FR23	717.5	39.0263	-0.7105
DEA5	1623	36.6406	-3.5710	FR24	1000.7	36.9178	-5.4984
DEB1	717	30.4163	2.2064	FR25	578.5	35.3476	0.5107
DEB2	264.5	27.3227	5.4179	FR26	639.7	36.3674	-0.8022
DEB3	981	34.4872	-1.8957	FR30	1492.6	40.0367	-9.7134
DECO	464.8	37.4714	-16.7558	FR41	904.6	33.8760	-3.6439
DED2	743.8	29.6917	-2.8087	FR42	809.4	38.1816	-1.5240
DED4	688.1	26.9450	-1.2953	FR43	468.6	34.3149	-1.5676
DED5	474.6	30.7257	-11.4894	FR51	1509.7	38.0740	-5.1852
DEEO	1048.9	26.4915	-0.6728	FR52	1336.1	35.4520	-6.3303

Table 6: values for certain economic variables in the initial period (continued)

Regions	Employment (,000)	Wages (,000)	Tax per capita	Regions	Employment (,000)	Wages (,000)	Tax per capita
FR53	714.1	33.6521	-2.7788	PT18	298.5	14.7598	-5.8608
FR61	1351.6	36.9430	-1.0702	PT20	99.2	16.3219	-6.2235
FR62	1243.7	38.0533	-5.1936	PT30	108.8	16.3767	-17.9137
FR63	295.9	32.8944	0.3624	RO00	8549.1	5.3487	-4.7475
FR71	2699.9	41.4589	-6.7661	ROW	942281.9	6.3787	-21.9740
FR72	537.3	35.2944	-0.4261	SE11	1133.4	57.6199	-32.2830
FR81	955.4	36.5596	-12.5510	SE12	750.4	43.4934	-10.3679
FR82	1955.2	40.4663	-2.1720	SE21	394.9	42.9335	-16.4701
FR83	62.2	76.1150	5.8688	SE22	672.4	43.0339	-14.3611
HRV	1524	13.2857	-4.5796	SE23	951.4	45.2112	-19.2227
HU00	3892.8	11.4695	-4.0549	SE31	387.3	40.2808	-14.9350
IE00	1888.5	37.0222	-12.2011	SE32	172.5	41.1574	-18.1878
ITC1	1770.7	28.0785	2.6194	SE33	242.2	44.0754	-19.6394
ITC2	54.7	29.5649	1.1561	SI01	473.5	16.2699	-6.0152
ITC3	603.1	28.4112	2.5062	SI02	432.4	23.9815	-8.1984
ITC4	4221.5	32.7454	3.3762	SK01	315.2	25.2848	-37.2071
ITF1	485.9	24.7781	0.5496	SK02	824.8	9.9025	-4.6217
ITF2	98.6	23.2282	-1.1462	SK03	563.9	10.0251	-3.7930
ITF3	1580.5	25.2469	1.0020	SK04	625.4	8.9685	-2.8448
ITF4	1158.4	25.0275	-1.9092	UKC1	491.7	17.5744	-3.1072
ITF5	178.6	23.4306	-1.7435	UKC2	641.4	18.3381	-4.3161
ITF6	518.2	24.3568	-5.9952	UKD1	240.1	17.3029	-5.7346
ITG1	1334.7	26.0958	-0.9188	UKD3	1215.3	20.4385	-5.6784
ITG2	546.3	24.2010	-1.0885	UKD4	639.2	18.0588	-5.2991
ITH1	243	34.1951	-149.0669	UKD6	431.8	20.0000	-482.5718
ITH2	229.2	31.3578	-133.8738	UKD7	657.2	18.0000	-192.0488
ITH3	2043.1	27.8717	-21.2817	UKE1	422.9	17.9032	-5.4246
ITH4	495.5	30.2206	-64.0954	UKE2	386.9	17.8377	-6.8607
ITH5	1904.1	29.6837	-19.8107	UKE3	621.8	16.2434	-4.0021
ITI1	1534.1	26.0740	-22.6776	UKE4	1006.7	20.3470	-5.9306
ITI2	349	24.1860	-80.4305	UKF1	973.3	18.1107	-4.7019
ITI3	615.7	24.4328	-62.6243	UKF2	816.7	20.1079	-5.2289
ITI4	2225.5	33.1702	-6.1929	UKF3	342.8	13.8482	-6.0697
LTU	1292.8	10.6252	-3.6102	UKG1	642.1	18.5413	-7.2492
LUX	238.7	94.9323	-29.9842	UKG2	754.6	15.9560	-5.0271
LVA	893.9	10.5386	-9.1278	UKG3	1136.4	20.7606	-5.1592
MLT	181.6	18.9572	-21.8877	UKH1	1155.3	19.0563	-6.9705
NL00	8285.3	39.1563	-15.0150	UKH2	885.8	23.2023	-5.7939
PL11	1247.7	6.8668	-1.8066	UKH3	839.2	16.7792	-4.3132
PL12	1044	6.1360	-10.7953	UKI1	1524.1	63.3986	-51.8633
PL21	1314.9	8.9553	-3.7728	UKI2	2238.5	19.7223	-4.3527
PL22	1903.3	10.4714	-6.6889	UKJ1	1184.5	30.0798	-10.9109
PL31	957.8	5.9883	-0.7577	UKJ2	1360.9	20.6045	-5.7982
PL32	800.1	7.5038	-0.5484	UKJ3	938.1	21.0874	-5.7748
PL33	554	6.1924	-1.1444	UKJ4	806.6	16.6803	-4.7454
PL34	453.3	7.1266	-0.9235	UKK1	1171.8	20.7576	-7.0298
PL41	1365.6	9.8957	-6.1769	UKK2	615.3	15.6705	-4.1230
PL42	572.4	9.2231	-3.3541	UKK3	238.8	13.0924	-3.5742
PL43	404.7	7.8447	-2.4368	UKK4	512.6	16.1075	-4.3383
PL51	1055.6	11.6458	-6.7876	UKL1	851.5	13.3424	-3.0907
PL52	346.1	9.0924	-3.1672	UKL2	535.7	18.6897	-6.4178
PL61	761.4	8.4268	-2.2920	UKM2	962.8	18.7273	-3.5270
PL62	528.7	7.4999	-1.8660	UKM3	991.2	19.9211	-2.4920
PL63	894.1	9.4477	-4.9896	UKM5	251.7	39.1981	-22.0718
PT11	1543.9	14.4577	-5.5697	UKM6	233.6	14.2053	-7.6387
PT15	186.9	14.6988	-9.9246	UKNO	797.2	15.9449	-3.0347
PT16	1059.2	12.8656	-5.9253				
PT17	1132.9	26.1299	-10.9246				

Table 7: values for certain disease-related variables in the initial period

Region	Date pandemic starts	Fraction non-telematic workers	Population	Infected	Region	Date pandemic starts	Workers face2face	Population	Infected
AT11	27-Mar-20	0.643	291942	103	DEF0	16-Mar-20	0.656	2881926	2471
AT12	19-Mar-20	0.636	1665753	1949	DEG0	21-Mar-20	0.661	2158128	2216
AT13	14-Mar-20	0.593	1867582	1853	DK01	28-Feb-20	0.599	1807404	5
AT21	30-Mar-20	0.634	561077	411	DK02	3-Mar-20	0.649	832553	4
AT22	17-Mar-20	0.645	1237298	2240	DK03	1-Mar-20	0.651	1217224	4
AT31	23-Mar-20	0.646	1465045	1532	DK04	15-Jul-20	0.654	1304253	1
AT32	26-Mar-20	0.619	549263	1098	DK05	8-Mar-20	0.659	587335	4
AT33	21-Mar-20	0.619	746153	2603	EE00	30-Mar-20	0.652	1315635	1611
AT34	29-Mar-20	0.640	388752	616	EL11	12-Oct-20	0.632	602799	4
BE10	10-Mar-20	0.606	1199095	4804	EL12	15-Jul-20	0.630	1880122	3
BE20	14-Mar-20	0.650	6526061	25756	EL13	10-Aug-20	0.635	271488	3
BE30	15-Mar-20	0.658	3626571	23733	EL14	29-Jul-20	0.637	725874	4
BG00	27-Mar-20	0.646	7101859	1337	EL21	28-Aug-20	0.630	335250	3
CYP	29-Mar-20	0.606	854802	328	EL22	9-Nov-20	0.588	205431	3
CZ01	24-Mar-20	0.590	1280508	2613	EL23	15-Aug-20	0.630	663970	3
CZ02	30-Mar-20	0.666	1338982	832	EL24	8-Sep-20	0.643	555761	3
CZ03	6-Apr-20	0.668	1217411	630	EL25	9-Aug-20	0.630	579182	3
CZ04	30-Mar-20	0.660	1118126	913	EL30	9-Nov-20	0.607	3773559	11
CZ05	1-Apr-20	0.672	1508527	426	EL41	14-Aug-20	0.598	203700	4
CZ06	1-Apr-20	0.662	1687764	734	EL42	11-Oct-20	0.554	338383	3
CZ07	30-Mar-20	0.666	1217623	439	EL43	9-Aug-20	0.580	632674	4
CZ08	30-Mar-20	0.662	1209879	604	ES11	15-Mar-20	0.640	2710216	4876
DE11	6-Mar-20	0.667	4098278	3280	ES12	18-Mar-20	0.632	1034302	4226
DE12	12-Mar-20	0.658	2779314	2525	ES13	20-Mar-20	0.635	581490	3846
DE13	8-Mar-20	0.667	2239734	3829	ES21	7-Mar-20	0.635	2167323	5877
DE14	15-Mar-20	0.668	1834567	5410	ES22	16-Mar-20	0.644	640353	6582
DE21	13-Mar-20	0.645	4633323	10328	ES23	11-Mar-20	0.648	312624	2601
DE22	16-Mar-20	0.665	1219397	5266	ES24	7-Mar-20	0.639	1316072	1332
DE23	15-Mar-20	0.662	1098378	6771	ES30	7-Mar-20	0.587	6476838	73177
DE24	15-Mar-20	0.662	1062394	3236	ES41	13-Mar-20	0.642	2435951	21224
DE25	19-Mar-20	0.653	1750059	6600	ES42	11-Mar-20	0.637	2040977	20921
DE26	11-Mar-20	0.660	1309209	2450	ES43	15-Mar-20	0.645	1077525	7275
DE27	13-Mar-20	0.663	1857991	2273	ES51	9-Mar-20	0.625	7441284	22909
DE30	17-Mar-20	0.620	3574830	6113	ES52	12-Mar-20	0.633	4935182	13246
DE40	24-Mar-20	0.639	2494648	4757	ES53	19-Mar-20	0.583	1150962	3553
DE50	25-Mar-20	0.642	678753	1018	ES61	13-Mar-20	0.630	8408976	11181
DE60	12-Mar-20	0.626	1810438	2122	ES62	22-Mar-20	0.649	1472991	3989
DE71	19-Mar-20	0.626	3951234	5456	ES63	4-Apr-20	0.637	85034	108
DE72	23-Mar-20	0.662	1043643	1030	ES64	3-Sep-20	0.639	84946	73
DE73	22-Mar-20	0.661	1218211	3269	ES70	16-Mar-20	0.590	2154978	3137
DE80	26-Mar-20	0.653	1610674	847	FI19	5-Mar-20	0.620	1380593	5986
DE91	17-Mar-20	0.659	1922674	3850	FI1B	26-Feb-20	0.653	1638293	5548
DE92	19-Mar-20	0.656	2139976	3143	FI1C	6-Mar-20	0.666	1159174	3869
DE93	25-Mar-20	0.660	1703945	1811	FI1D	3-Mar-20	0.669	1781976	3197
DE94	14-Mar-20	0.665	2506155	2101	FI20	21-Mar-20	0.661	29214	334
DEA1	11-Mar-20	0.637	5190790	3618	FR10	18-Mar-20	0.630	12174880	84443
DEA2	6-Mar-20	0.610	4439416	4521	FR21	19-Mar-20	0.660	1334453	5846
DEA3	17-Mar-20	0.660	2619376	4106	FR22	18-Mar-20	0.659	1934171	12914
DEA4	17-Mar-20	0.664	2054205	1620	FR23	19-Mar-20	0.656	1865332	3153
DEA5	18-Mar-20	0.668	3586313	4113	FR24	22-Mar-20	0.651	2582302	7177
DEB1	16-Mar-20	0.659	1657077	1421	FR25	23-Mar-20	0.653	1477290	2811
DEB2	25-Mar-20	0.657	528728	587	FR26	18-Mar-20	0.656	1637366	6448
DEB3	20-Mar-20	0.665	2045138	2280	FR30	18-Mar-20	0.648	4087132	7110
DEC0	17-Mar-20	0.635	996651	2914	FR41	18-Mar-20	0.656	2330674	24535
DED2	19-Mar-20	0.634	1600155	1517	FR42	18-Mar-20	0.650	1888937	34338
DED4	21-Mar-20	0.641	1454144	3704	FR43	18-Mar-20	0.658	1179900	7869
DED5	26-Mar-20	0.623	1027484	669	FR51	21-Mar-20	0.650	3765798	6748
DEE0	20-Mar-20	0.662	2236252	1689	FR52	18-Mar-20	0.645	3323130	3074

Table 7: values for certain disease-related variables in the initial period (continued)

Region	Date pande_	Fraction non-	Population	Infected	Region	Date pande_	Workers	Population	Infected
	mic starts	telematic workers				mic starts	face2face		
FR53	21-Mar-20	0.657	1811206	2696	PT18	24-Jun-20	0.666	718087	788
FR61	22-Mar-20	0.652	3422179	4015	PT20	10-Apr-20	0.667	245283	377
FR62	19-Mar-20	0.637	3046465	1854	PT30	13-Oct-20	0.652	254876	0
FR63	22-Mar-20	0.658	735908	928	RO00	21-Mar-20	0.651	19643949	8707
FR71	18-Mar-20	0.641	6621564	20221	ROW	25-Feb-20	0.635	1719968968	340
FR72	26-Mar-20	0.649	1365263	1584	SE11	26-Mar-20	0.580	2269060	25240
FR81	18-Mar-20	0.681	2815936	4746	SE12	26-Mar-20	0.623	1664145	7369
FR82	19-Mar-20	0.639	5047942	8072	SE21	26-Mar-20	0.635	847667	1350
FR83	19-Mar-20	0.651	334283	1388	SE22	26-Mar-20	0.615	1483018	1042
HRV	27-Mar-20	0.628	4154213	1139	SE23	26-Mar-20	0.616	1992116	2741
HU00	20-Mar-20	0.659	12797637	1440	SE31	26-Mar-20	0.629	848451	2820
IE00	21-Mar-20	0.611	9568766	7688	SE32	7-Apr-20	0.614	374245	1370
ITC1	5-Mar-20	0.653	4392526	10749	SE33	5-Apr-20	0.623	516451	1578
ITC2	17-Mar-20	0.657	126883	3391	SI01	23-Mar-20	0.670	1091159	1414
ITC3	4-Mar-20	0.652	1565307	5372	SI02	28-Mar-20	0.643	974736	984
ITC4	20-Feb-20	0.650	10019166	65345	SK01	18-Aug-20	0.614	641892	22
ITF1	14-Mar-20	0.658	1322247	4935	SK02	15-Mar-20	0.665	1830751	3
ITF2	19-Mar-20	0.661	310449	464	SK03	25-Aug-20	0.667	1342287	9
ITF3	13-Mar-20	0.659	5839084	5535	SK04	10-Aug-20	0.669	1620413	9
ITF4	7-Mar-20	0.667	4063888	1735	UKC1	15-Mar-20	0.627	1194437	5
ITF5	26-Mar-20	0.668	570365	858	UKC2	13-Mar-20	0.624	1446249	5
ITF6	18-Mar-20	0.679	1965128	2213	UKD1	9-Mar-20	0.631	498641	4
ITG1	16-Mar-20	0.665	5056641	4126	UKD3	9-Mar-20	0.620	2789735	6
ITG2	20-Mar-20	0.665	1653135	2285	UKD4	13-Mar-20	0.631	1487102	6
ITH1	13-Mar-20	0.635	524256	3648	UKD6	15-Mar-20	0.592	924261	5
ITH2	14-Mar-20	0.635	538604	6967	UKD7	12-Mar-20	0.598	1541473	6
ITH3	2-Mar-20	0.640	4907529	4053	UKE1	18-Mar-20	0.635	929189	4
ITH4	9-Mar-20	0.636	1217872	3352	UKE2	15-Mar-20	0.626	818141	4
ITH5	28-Feb-20	0.641	4448841	12423	UKE3	8-Mar-20	0.627	1389426	5
ITI1	11-Mar-20	0.639	3742437	8173	UKE4	12-Mar-20	0.622	2301000	5
ITI2	19-Mar-20	0.637	888908	2023	UKF1	6-Mar-20	0.631	2187643	5
ITI3	3-Mar-20	0.636	1538055	5090	UKF2	10-Mar-20	0.627	1812852	5
ITI4	7-Mar-20	0.639	5898124	3241	UKF3	16-Mar-20	0.639	747996	4
LTU	25-Mar-20	0.681	5695808	568	UKG1	9-Mar-20	0.631	1338055	5
LUX	18-Mar-20	0.598	590667	1509	UKG2	10-Mar-20	0.631	1613788	5
LVA	11-Apr-20	0.649	1950116	499	UKG3	6-Mar-20	0.623	2883905	6
MLT	10-Apr-20	0.599	460297	99	UKH1	10-Mar-20	0.628	2493326	5
NL00	9-Mar-20	0.636	21063191	15453	UKH2	8-Mar-20	0.622	1841673	5
PL11	2-Apr-20	0.663	4943240	466	UKH3	10-Mar-20	0.627	1813609	6
PL12	25-Mar-20	0.611	10682968	2133	UKI1	1-Mar-20	0.593	3206667	6
PL21	1-Apr-20	0.652	3339803	730	UKI2	4-Mar-20	0.612	5267064	12
PL22	28-Mar-20	0.657	4510528	2415	UKJ1	5-Mar-20	0.612	2385514	5
PL31	29-Mar-20	0.673	4225574	369	UKJ2	7-Mar-20	0.617	2871387	5
PL32	1-Apr-20	0.671	4169444	630	UKJ3	6-Mar-20	0.617	1973952	5
PL33	15-Apr-20	0.669	2475036	288	UKJ4	11-Mar-20	0.627	1824794	6
PL34	15-Apr-20	0.675	2313894	74	UKK1	9-Mar-20	0.621	2474784	5
PL41	31-Mar-20	0.669	3457473	2145	UKK2	17-Mar-20	0.630	1322286	4
PL42	18-Apr-20	0.666	1681246	547	UKK3	14-Mar-20	0.630	560526	4
PL43	22-Jul-20	0.672	1004892	497	UKK4	11-Mar-20	0.628	1180517	3
PL51	24-Mar-20	0.659	2866218	649	UKL1	10-Mar-20	0.630	1960764	6
PL52	6-Apr-20	0.672	950710	782	UKL2	9-Mar-20	0.628	1158491	6
PL61	7-Apr-20	0.669	2060575	979	UKM2	9-Mar-20	0.624	4176323	5
PL62	10-Aug-20	0.677	1410641	232	UKM3	8-Mar-20	0.625	4712134	5
PL63	21-Apr-20	0.656	2285800	1012	UKM5	19-Jul-20	0.614	491323	2
PT11	20-Mar-20	0.646	3584575	7664	UKM6	13-Mar-20	0.634	469420	4
PT15	1-Apr-20	0.641	441469	403	UKN0	15-Mar-20	0.630	2764538	4
PT16	20-Mar-20	0.656	2243934	3630					
PT17	20-Mar-20	0.603	2821349	2762					

Table 8: results

Region code	Region name	Deaths during first wave		Predicted deaths		Predicted deaths with ρ constant		
		Total	per 100,000	Total	% Geografic	Total	% increase	Lives saved*
EU27	European Union	133063	28	107112	10.2%	4545222	4143%	202
UK	United Kingdom	40672	57	30571	9.7%	1248078	3983%	1718
UKC1	Tees Valley and Durham	1037	87	737	9.9%	19622	2564%	1581
UKC2	Northumberland and Tyne and Wear	1095	76	827	12.8%	22484	2619%	1497
UKD1	Cumbria	382	77	323	8.6%	6302	1854%	1199
UKD3	Greater Manchester	2587	93	1660	9.8%	63906	3749%	2231
UKD4	Lancashire	1016	68	762	9.4%	22772	2889%	1480
UKD6	Cheshire	829	90	505	9.1%	21494	4158%	2271
UKD7	Merseyside	1283	83	920	10.1%	29038	3057%	1824
UKE1	East Yorkshire and Northern Lincolnshire	546	59	409	11.7%	10115	2374%	1045
UKE2	North Yorkshire	464	57	353	11.5%	13982	3865%	1666
UKE3	South Yorkshire	1120	81	788	8.7%	24589	3021%	1713
UKE4	West Yorkshire	1440	63	1052	11.2%	46595	4330%	1979
UKF1	Derbyshire and Nottinghamshire	1416	65	977	10.6%	49536	4970%	2220
UKF2	Leicestershire, Rutland and Northamptonshire	1250	69	863	8.6%	35603	4026%	1916
UKF3	Lincolnshire	262	35	237	10.5%	6585	2680%	849
UKG1	Herefordshire, Worcestershire and Warwickshire	942	70	651	11.6%	25729	3852%	1874
UKG2	Shropshire and Staffordshire	1121	69	815	9.4%	29821	3560%	1797
UKG3	West Midlands	2496	87	1737	13.4%	63443	3553%	2140
UKH1	East Anglia	1248	50	996	10.2%	41422	4060%	1621
UKH2	Bedfordshire and Hertfordshire	1414	77	1051	9.7%	27648	2532%	1444
UKH3	Essex	1443	80	992	11.3%	38064	3737%	2044
UKI1	Inner London - West	2063	64	1891	9.1%	58138	2974%	1754
UKI2	Inner London - East	4155	79	2849	19.6%	116507	3989%	2158
UKJ1	Berkshire, Buckinghamshire and Oxfordshire	1138	48	710	15.8%	64021	8921%	2654
UKJ2	Surrey, East and West Sussex	1544	54	1144	13.5%	50870	4346%	1732
UKJ3	Hampshire and Isle of Wight	1001	51	772	11.9%	31357	3960%	1549
UKJ4	Kent	1254	69	879	7.8%	31617	3498%	1684
UKK1	Gloucestershire, Wiltshire and Bristol/Bath area	1088	44	859	15.8%	41523	4731%	1643
UKK2	Dorset and Somerset	256	19	271	11.2%	12210	4407%	903
UKK3	Cornwall and Isles of Scilly	247	44	245	8.5%	7465	2943%	1288
UKK4	Devon	262	22	261	16.8%	15294	5760%	1273
UKL1	West Wales and The Valleys	975	50	776	9.8%	27188	3402%	1347
UKL2	East Wales	576	50	462	9.7%	14964	3142%	1252
UKM2	Eastern Scotland	1002	24	952	17.0%	54301	5603%	1277
UKM3	South Western Scotland	1268	27	1237	10.7%	82975	6609%	1735
UKM5	North Eastern Scotland	139	28	148	7.8%	4378	2851%	861
UKM6	Highlands and Islands	150	32	145	9.4%	5164	3454%	1069
UKN0	Northern Ireland (UK)	163	6	318	14.2%	31357	9763%	1123

* Lives saved per 100,000 inhabitants

Table 9: intra- and inter-regional trade for the UK NUTS2 regions

Region code	Region name	Domestic	Rest of UK	EU27	ROW
UKC1	Tees Valley and Durham	0.3077	0.6048	0.0684	0.0192
UKC2	Northumberland and Tyne and Wear	0.3759	0.5335	0.0767	0.0139
UKD1	Cumbria	0.3565	0.5788	0.0600	0.0047
UKD3	Greater Manchester	0.4075	0.5355	0.0444	0.0126
UKD4	Lancashire	0.3055	0.6381	0.0498	0.0066
UKD6	Cheshire	0.5960	0.2538	0.0435	0.1067
UKD7	Merseyside	0.5622	0.3392	0.0608	0.0378
UKE1	East Yorkshire and Northern Lincolnshire	0.3799	0.5651	0.0486	0.0064
UKE2	North Yorkshire	0.3473	0.6043	0.0420	0.0064
UKE3	South Yorkshire	0.3082	0.6175	0.0705	0.0038
UKE4	West Yorkshire	0.3824	0.5594	0.0514	0.0069
UKF1	Derbyshire and Nottinghamshire	0.3326	0.6125	0.0435	0.0113
UKF2	Leicestershire, Rutland and Northamptonshire	0.3917	0.5518	0.0469	0.0096
UKF3	Lincolnshire	0.2870	0.6605	0.0471	0.0055
UKG1	Herefordshire, Worcestershire and Warwickshire	0.3577	0.5881	0.0445	0.0097
UKG2	Shropshire and Staffordshire	0.3399	0.6222	0.0336	0.0043
UKG3	West Midlands	0.3854	0.5293	0.0609	0.0244
UKH1	East Anglia	0.4131	0.5061	0.0470	0.0338
UKH2	Bedfordshire and Hertfordshire	0.3542	0.5449	0.0715	0.0294
UKH3	Essex	0.3100	0.5926	0.0712	0.0262
UKI1	Inner London - West	0.4516	0.3885	0.0786	0.0814
UKI2	Inner London - East	0.3336	0.4973	0.0755	0.0936
UKJ1	Berkshire, Buckinghamshire and Oxfordshire	0.4515	0.4487	0.0618	0.0380
UKJ2	Surrey, East and West Sussex	0.3566	0.5038	0.0703	0.0693
UKJ3	Hampshire and Isle of Wight	0.4294	0.5032	0.0404	0.0271
UKJ4	Kent	0.3450	0.5663	0.0561	0.0326
UKK1	Gloucestershire, Wiltshire and Bristol/Bath area	0.3963	0.5291	0.0412	0.0334
UKK2	Dorset and Somerset	0.3043	0.6347	0.0387	0.0223
UKK3	Cornwall and Isles of Scilly	0.3592	0.5865	0.0446	0.0097
UKK4	Devon	0.3456	0.5941	0.0380	0.0223
UKL1	West Wales and The Valleys	0.3028	0.6213	0.0464	0.0295
UKL2	East Wales	0.3308	0.6266	0.0352	0.0073
UKM2	Eastern Scotland	0.4013	0.5328	0.0322	0.0337
UKM3	South Western Scotland	0.4299	0.5073	0.0323	0.0304
UKM5	North Eastern Scotland	0.6156	0.3434	0.0347	0.0063
UKM6	Highlands and Islands	0.3984	0.5451	0.0469	0.0096
UKN0	Northern Ireland (UK)	0.4262	0.4928	0.0480	0.0330

Table 10: Additional results with ρ constant

Region code	Region name	Predicted deaths with ρ constant in EU27			Predicted deaths with ρ constant in UK		
		Total	% increase	Lives saved*	Total	% increase	Lives saved*
EU27	European Union	4485729	4088%	200	157732	47%	2
UK	United Kingdom	55005	80%	34	1234811	3939%	1700
UKC1	Tees Valley and Durham	1146	56%	34	19367	2530%	1560
UKC2	Northumberland and Tyne and Wear	1314	59%	34	22135	2577%	1473
UKD1	Cumbria	609	89%	57	6137	1803%	1166
UKD3	Greater Manchester	2185	32%	19	63746	3739%	2225
UKD4	Lancashire	1178	55%	28	22501	2854%	1462
UKD6	Cheshire	733	45%	25	21427	4145%	2264
UKD7	Merseyside	1424	55%	33	28803	3032%	1809
UKE1	East Yorkshire and Northern Lincolnshire	791	93%	41	9714	2276%	1001
UKE2	North Yorkshire	661	87%	38	13801	3814%	1644
UKE3	South Yorkshire	1189	51%	29	24371	2993%	1697
UKE4	West Yorkshire	1541	47%	21	46383	4310%	1970
UKF1	Derbyshire and Nottinghamshire	1572	61%	27	49362	4952%	2212
UKF2	Leicestershire, Rutland and Northamptonshire	1459	69%	33	35357	3998%	1903
UKF3	Lincolnshire	616	160%	51	6282	2552%	808
UKG1	Herefordshire, Worcestershire and Warwickshire	1089	67%	33	25535	3822%	1860
UKG2	Shropshire and Staffordshire	1249	53%	27	29621	3535%	1785
UKG3	West Midlands	2370	36%	22	63226	3540%	2132
UKH1	East Anglia	2096	110%	44	40850	4003%	1598
UKH2	Bedfordshire and Hertfordshire	1694	61%	35	27255	2495%	1423
UKH3	Essex	1878	89%	49	37781	3709%	2028
UKI1	Inner London - West	3087	63%	37	57793	2956%	1743
UKI2	Inner London - East	4202	47%	26	116046	3973%	2149
UKJ1	Berkshire, Buckinghamshire and Oxfordshire	1302	83%	25	63897	8903%	2649
UKJ2	Surrey, East and West Sussex	2075	81%	32	50388	4304%	1715
UKJ3	Hampshire and Isle of Wight	1427	85%	33	30980	3911%	1530
UKJ4	Kent	1710	95%	46	31275	3459%	1666
UKK1	Gloucestershire, Wiltshire and Bristol/Bath area	1398	63%	22	41123	4685%	1627
UKK2	Dorset and Somerset	937	246%	50	11700	4219%	864
UKK3	Cornwall and Isles of Scilly	597	143%	63	7280	2867%	1255
UKK4	Devon	728	179%	40	14927	5620%	1242
UKL1	West Wales and The Valleys	1442	86%	34	26730	3343%	1324
UKL2	East Wales	841	82%	33	14680	3080%	1227
UKM2	Eastern Scotland	2262	138%	31	53068	5474%	1248
UKM3	South Western Scotland	3396	175%	46	82058	6535%	1715
UKM5	North Eastern Scotland	401	170%	51	4168	2709%	818
UKM6	Highlands and Islands	503	246%	76	4893	3268%	1011
UKN0	Northern Ireland (UK)	1903	499%	57	30150	9384%	1079

* Lives saved per 100,000 inhabitants